

Copyright is owned by the Author of the thesis. Permission is given for a copy to be downloaded by an individual for the purpose of research and private study only. The thesis may not be reproduced elsewhere without the permission of the Author.

127
6139

**ADSORPTION OF PENTACHLOROPHENOL
ONTO ACTIVATED CARBON IN A FIXED BED**

A thesis presented in partial fulfilment of the requirements
for the degree of
Master of Technology in Environmental Engineering
at Massey University

Andrew James Slaney

1995

ABSTRACT

The adsorption of pentachlorophenol (PCP) from water onto granular activated carbon (GAC) was studied. Equilibrium and kinetic behaviour was studied, and the results used to predict fixed bed adsorber behaviour.

Batch equilibrium tests showed that the adsorption capacity of activated carbon for PCP is best represented by the Freundlich isotherm, with constants of $K = 95$ and $1/n = 0.18$. Batch adsorption kinetics experiments were conducted in a spinning basket reactor. Surface diffusion and external film transfer coefficients were determined by fitting the homogeneous surface diffusion model (HSDM) to the experimental batch adsorption data. A surface diffusion coefficient value of 2.26×10^{-9} cm/s was calculated using this method, which was similar to surface diffusion coefficients for similar compounds found by other investigators.

Using equilibrium and kinetic parameters, the HSDM was used to predict bench scale fixed bed adsorber breakthrough curves at varying flow rates. A correlation was used to calculate the film transfer coefficient. There was a good agreement between the experimental breakthrough curves and those predicted by the model. By varying parameters in the model it was found that the adsorption rate in the PCP-activated carbon system was primarily limited by surface diffusion. The homogeneous surface diffusion model was shown to be effective in predicting breakthrough of PCP and could conceivably be used to predict full scale adsorber performance or to aid pilot plant studies.

ACKNOWLEDGEMENTS

I would like to thank my supervisor, Professor Rao Bhamidimarri for his advice, Don McClean and John Alger for their help in the workshop, and Shridar Sursala and Vijay Bhaskar for their assistance with the computer programs. Last but not least I would like to thank my friends and family for their support and encouragement.

CONTENTS

Abstract	i
Acknowledgements	ii
List of Figures	1
List of Tables	3
1. Introduction	4
2. Literature Review	
2.1 Activated carbon: Applications	11
2.2 Types of Adsorbent	12
2.3 Contacting systems	13
2.4 Adsorption in Fixed Beds	15
2.5 Adsorption System Design	17
2.6 Adsorption Phenomena	20
2.7 Equilibrium Isotherm Models	21
2.8 Equilibrium Studies	23
2.9 Adsorption Kinetics	24
2.10 Modelling Fixed Bed Adsorbers	29
3. Materials and Methods	32
4. Equilibrium Studies	
4.1 Preliminary Studies	36
4.2 Equilibrium Isotherms	37
5. Adsorption Kinetics	
5.1 Homogeneous Surface Diffusion Model	42
5.2 Model equations	43
5.3 Results and Discussion	46

6. Column Studies	
6.1 Fixed Bed Adsorbers	55
6.2 Fixed Bed Adsorber Operation	56
6.3 Fixed Bed Adsorber Design	57
6.4 HSDM Applied to Fixed Bed Adsorbers	58
6.5 Model Parameter Determination	62
6.6 Experimental and Predicted Breakthrough Curves	65
6.7 Applications of the Model	72
7. Conclusions	74
List of Symbols	76
References	78
Appendix 1: Isotherm Experimental Data	87
Appendix 2: Kinetic Experimental Data	91
Appendix 3: Column Experimental Data	93

LIST OF FIGURES

Figure 1.1:	Physical Characteristics of an Activated Carbon Particle	5
Figure 1.2:	Downflow Fixed-Bed Pressure Adsorber	8
Figure 2.1:	Batch Adsorption Configurations	14
Figure 2.2:	Breakthrough Curve for a Fixed Bed Adsorber	16
Figure 2.3:	Bed Depth Service Time Curve for a Fixed Bed Adsorber	18
Figure 2.4:	Types of Adsorption Equilibrium Isotherm	21
Figure 2.5:	Transport Steps in Adsorption by Porous Adsorbents	25
Figure 2.6:	Material Balances in a Fixed Bed Adsorber	30
Figure 3.1:	Rotating Wire Basket Adsorption Batch Reactor	33
Figure 3.2:	Adsorption Column Experimental Setup	34
Figure 4.1:	Equilibrium Time Test	36
Figure 4.2:	Equilibrium Isotherm, Initial PCP Concentration = 250 ppm	37
Figure 4.3:	Equilibrium Isotherm, Initial PCP Concentration = 500 ppm	38
Figure 4.4:	Equilibrium Isotherm, Initial PCP Concentration = 250 ppm	38
Figure 4.5:	Equilibrium Isotherm, Initial PCP Concentration = 500 ppm	39
Figure 4.6:	Equilibrium Isotherm, Initial PCP Concentration = 500, 250 ppm	39
Figure 5.1:	Mechanisms and Assumptions Incorporated in the HSDM	42
Figure 5.2:	Solute Uptake Curves for Various Stirrer speeds	46
Figure 5.3:	Initial Solute Uptake for Stirrer Speed of 180 rpm	48
Figure 5.4:	Initial Solute Uptake for Stirrer Speed of 390 rpm	48
Figure 5.5:	Initial Solute Uptake for Stirrer Speed of 560 rpm	49
Figure 5.6:	Initial Solute Uptake for Stirrer Speed of 760 rpm	49
Figure 5.7:	Solute Uptake Plot and HSDM Solution, Stirrer Speed 180 rpm	51
Figure 5.8:	Solute Uptake Plot and HSDM Solution, Stirrer Speed 390 rpm	51

Figure 5.9:	Solute Uptake Plot and HSDM Solution, Stirrer Speed 560 rpm	52
Figure 5.10:	Solute Uptake Plot and HSDM Solution, Stirrer Speed 760 rpm	52
Figure 6.1:	PCP Breakthrough Curve, Flow Rate = 2.80 ml/min	66
Figure 6.2:	PCP Breakthrough Curve, Flow Rate = 5.07 ml/min	67
Figure 6.3:	PCP Breakthrough Curve, Flow Rate = 6.15 ml/min	67
Figure 6.4:	Effect of Flow Rate on the Breakthrough Curve	68
Figure 6.5:	Effect of Hydraulic Loading Rate on Breakthrough and Exhaustion Throughputs	69
Figure 6.6:	Effect of Different k_1 Correlations on the Breakthrough Curve	71
Figure 6.7:	Effect of D_s on the Breakthrough Curve	72

LIST OF TABLES

Table 4.1:	Freundlich Isotherm Coefficients	40
Table 4.2:	Freundlich Coefficients for Phenolic Compounds in Water	41
Table 5.1:	Film Transfer Coefficients Calculated From Initial Slope Data	47
Table 5.2:	HSDM Input Parameters and Surface Diffusion Coefficients	50
Table 5.3:	Literature Values of k_1 and D_s	53
Table 6.1:	HSDM Dimensionless Groups	61
Table 6.2:	Fixed Bed Model Input Parameters	65

1. INTRODUCTION

Adsorption is a process in which a soluble contaminant, or adsorbate, is transferred from a liquid phase to the surface of a solid phase, or adsorbent. This transfer is caused by attractive forces between the molecules on the solid surface and the contaminant in solution, and is further enhanced by a lack of affinity of the contaminant for the solution.

Although these naturally occurring forces will cause dissolved molecules to accumulate on just about any solid surface, materials with a large surface area to mass ratio are necessary for practical adsorption applications. Granular activated carbon (GAC) is the most common adsorbent used in water and wastewater treatment, due to its applicability to a broad range of different contaminants found in water and wastewater. GAC can be manufactured from almost any carbonaceous raw material, but most commercial GAC's are made from bituminous coal and coconut shell. The manufacturing process involves particle forming and sizing followed by controlled charring and high temperature steam activation. The resulting particle structure is highly porous, with a range of macro and micropores reaching down to molecular dimensions (Figure 1.1). This leads to a very high surface area, usually around 1500 m² per g of adsorbent (Graham and Ramaratnam, 1993). Surface area, pore size and surface functional groups are important properties in determining a GAC's adsorptive capacity, and depend on the raw material and manufacturing process employed (Weber, 1984).

The scientific study of adsorption processes is a relatively recent development compared to its use in water purification. Recorded use of charcoal to improve

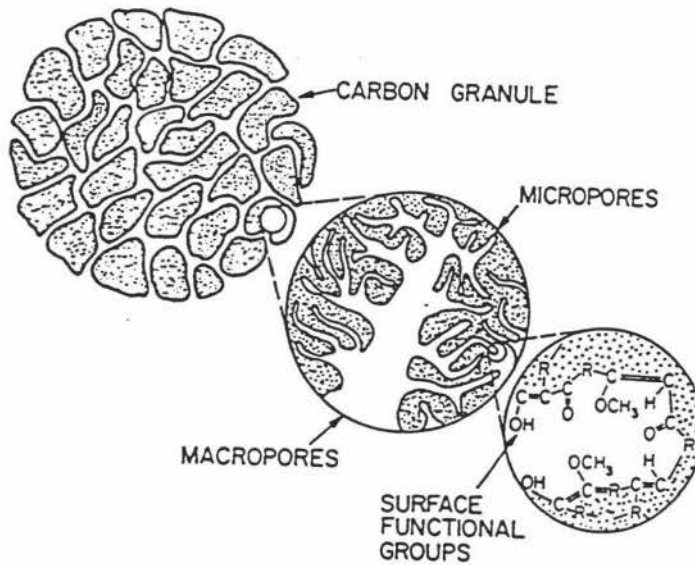


Figure 1.1: Physical Characteristics of an Activated Carbon Particle (Weber, 1984)

water taste and odour date back to 1500 BC (Weber, 1984), but it was not until the late eighteenth century that the phenomenon of adsorption was recognised, and rigorous and quantitative theories were not developed until the first quarter of this century.

Applications of activated carbon adsorption processes beyond the control of taste and odour of drinking water have expanded greatly in the last thirty years due to increased contamination of water supplies by synthetic organic contaminants (SOCs), particularly in the USA and Europe. As many of these chemicals are recalcitrant to conventional biological treatment processes, activated carbon adsorption is often the most suitable option for their removal. The success of activated carbon adsorption in removing SOCs in the USA led to its use as the "Best Available Technology" benchmark for SOC control in the Safe Drinking Water Act Amendments of 1986 (Stenzel, 1993).

Today activated carbon adsorption is used in a variety of water and wastewater treatment applications. The most common use in municipal wastewater treatment is the use of GAC adsorbers as a tertiary polishing step following secondary biological treatment. However other applications include treating industrial effluents prior to discharge to sewer, as an addition to the aeration basins of activated sludge systems, as a support medium for attached growth processes, as a means of byproduct recovery, and as a means of cleaning up contaminated groundwater and landfill leachate (Stenzel and Merz, 1989).

New Zealand, with its low population and industrial density, has limited experience with activated carbon adsorption or SOC water contamination compared to the USA or Europe. However groundwater contamination is an increasing concern, and the extent of contamination is yet to be determined accurately. A report commissioned by the Ministry for the Environment in 1992 estimated that the number of locations where site contamination may have occurred was approximately 7800, roughly twenty percent of which are thought to pose a high risk to the public and the environment (Worley, 1992).

Pesticides are one group of SOCs that pose a high risk to the public and the environment as they are not only toxic but persistent and bioaccumulative. A particular source of concern in New Zealand since 1988 has been the contamination of timber treatment sites with pentachlorophenol (PCP). PCP was widely used in the timber industry as an anti-fungal agent for forty years up until 1988 when it was voluntarily withdrawn from use by the industry in recognition of overseas evidence of potential occupational health risks. It is estimated that the total PCP usage during this period was approximately 5000 tonnes (MFE, 1992). PCP is a highly toxic

chemical, and industrial grades used in the timber industry have been found to contain trace amounts of highly toxic polychlorinated dibenzo dioxins and furans (Jorens and Schepens, 1993).

In December 1990 the Ministry for the Environment convened a national task group to assess the significance of contamination of timber treatment sites. The group found that there were approximately 600 sites around the country where PCP may have been used and released into the soil. In order to gauge the extent of possible site contamination, the country's largest user of PCP, the Waipa timber treatment plant near Rotorua, was investigated. "Significant" concentrations of PCP, dioxins and furans were found in soils around the site, as well as in the groundwater, stormwater drains and the nearby Waipa stream. PCP and dioxins were also found in the biota and sediments of Lake Rotorua, in levels "comparable to overseas bodies located in heavily industrialised areas" (MFE, 1992).

Since the task group reported its findings in December 1992 approximately ten timber treatment sites around New Zealand have experienced some form of cleanup activity (Drent, 1994). The Australian and New Zealand Guidelines for the Assessment and Management of Contaminated Sites (ANZECC, 1992) provide a systematic framework for site investigation and cleanup. Although not commonly used in New Zealand to date, the use of activated carbon has been proven overseas as an efficient means of cleaning up contaminated waters from timber treatment sites (Dahab and Riley, 1991).

There are a number of configurations for contacting activated carbon with a water or wastewater in a treatment process. Plug-flow contactors are most commonly used

in water and wastewater treatment, the most common configuration being the downflow fixed bed pressure system, as shown in Figure 1.2. An advantage of the

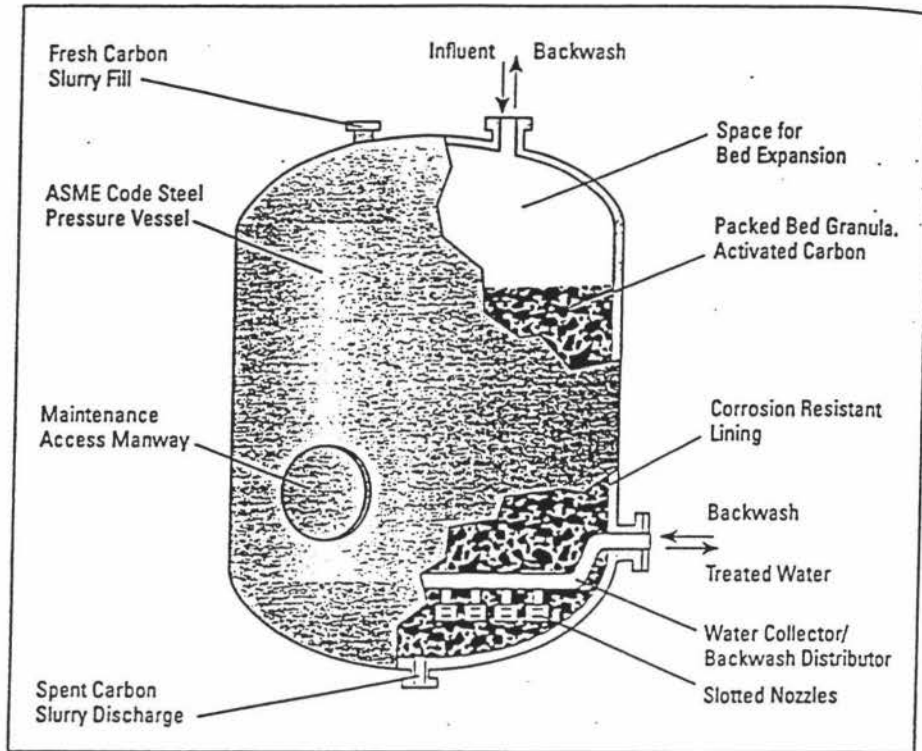


Figure 1.2: Downflow Fixed-Bed Pressure Adsorber (Stenzel, 1993)

pressure adsorber system is that the water does not need to be repumped after treatment. For example, many groundwater treatment adsorbers are placed between the well pump and downstream equipment and operate along with the well in an on-off mode (Stenzel, 1993). Also, beds may be operated in parallel or series and backwashing is possible. Gravity flow adsorbers are often used for applications that have low contact times and high flow rates, such as municipal water treatment plants (Culp and Clark, 1983). Batch reactor or continuous stirred-tank reactor configurations are generally used only in powdered activated carbon (PAC) applications where pressure drop through a fixed-bed would be prohibitive.

Whatever the configuration used, an essential element in the design and operation

of efficient adsorption systems is an accurate understanding of the underlying process. Mathematical models have proven to be useful in this regard. For example models have been applied to fixed bed systems in order to predict the appearance of contaminants from the adsorbent bed effluent (the breakthrough curve).

As with any modelling effort, the physical properties and characteristics of the system must first be defined. For an adsorption system this involves determining the equilibrium capacity of the adsorbent for the contaminant of interest, and the kinetic properties of the system. Mass balances can then be applied to the system and the resulting equations solved numerically. A number of different models have been successfully applied to adsorption systems, the differences largely centring on how the transport of solute inside the adsorbent particle is described.

At present, modelling of adsorption systems provides a means for interpreting bench scale data and for the translation of that data to the design of appropriate pilot programs. It is unrealistic in most wastewater applications to use models for the direct design of full scale adsorbers due to the complexity and variability of most wastewater applications. Models, however, can enable pilot test programs to be used primarily for design verification rather than preliminary data gathering. Also, once verified on the pilot plant, the model can be used to predict adsorber performance under various conditions. This can save a considerable amount of time and money.

The purpose of this study was to investigate the adsorption of PCP onto activated carbon, with a view to aiding any future pilot studies or adsorber design. Adsorption equilibria and kinetics were studied in order to determine parameters necessary to construct a mathematical model of the process, and bench scale column

experiments were conducted to test the accuracy of the model. Once verified, the model, rather than expensive pilot studies, can be used to predict adsorber performance.

2. LITERATURE REVIEW

2.1 Activated Carbon: Applications in Water and Wastewater Treatment

The use of activated carbon adsorption has evolved from applications for taste and odour control in drinking water to a range of uses in the water and wastewater treatment industries. Powdered activated carbon (PAC) has traditionally been added prior to clarification in order to remove taste and odour from public water supplies. However fixed bed granular activated carbon (GAC) installations are becoming more common in water treatment applications in the USA and Europe due to the increasing occurrence of trace organic contaminants in water supplies (Culp and Clark, 1983). Some water treatment plants replace sand or other filter media with GAC, while in other instances post-filter GAC beds are used (Weber and Smith, 1986). Adsorption technology has also been found to be effective in groundwater cleanup operations, including the treatment of drinking and process waters, treatment of waters for artificial recharge of aquifers, and aquifer decontamination by treatment of water from purge wells (O'Brien and Fisher, 1983, Stenzel and Merz, 1989). In such applications the use of pre-aeration to remove volatile organics prior to GAC treatment has shown to extend adsorber column runs significantly (McKinnon and Dyksen, 1984).

The chemical process industries use activated carbon for a diverse range of process water treatment applications, such as dechlorination of disinfected water supplies prior to reuse, removal of trace organic contaminants for protection of resin beds, treatment of steam for recycle, and removal of organic contaminants from water sources prior to plant use (Stenzel, 1993).

The application of adsorption technology for pollution control usually deals with the removal of organic compounds. Volatile organic compounds (VOC's), pesticides, PCB's, phenolics and chlorinated phenolics are typical adsorbates. In general, any organic compound having a molecular weight greater than 45 is likely to be a good candidate for activated carbon treatment (Noll *et al*, 1992). The most effective applications of GAC technology in municipal wastewater treatment have been in a tertiary mode that follows secondary biological treatment. In this configuration GAC serves a polishing role, removing trace amounts of biologically resistant contaminants prior to discharge into the environment. An alternative application is in independent physicochemical treatment (IPCT) where GAC is used to treat raw clarified wastewater which has not undergone prior biological treatment. IPCT is an attractive option for removing toxic organics from industrial effluents prior to discharge to the municipal sewer (Weber and Smith, 1986). A relatively new application is the addition of powdered activated carbon to the aeration tanks of activated sludge plants (PACT process). This process has been shown to be effective in assisting the biological assimilation of toxic organics in industrial effluents (O'Brien, 1992, Maroney *et al*, 1992).

2.2 Types of Adsorbent

The physicochemical nature of an adsorbent can have profound effects on both its rate and capacity for adsorption. Activated carbon is by far the most common adsorbent used in water and wastewater treatment applications, due to its high adsorptive capacity for a wide range of contaminants. Commercial activated carbons can be prepared from a wide variety of raw materials, including wood, lignite, coal, bone, petroleum residues and nut shells (Weber, 1972).

Irrespective of the raw material, two steps are common in the manufacture of all activated carbons. In the first step, carbonization, the raw material is pyrolysed to a carbonaceous residue which has a graphite-like structure. The second step, activation, is designed to develop a porous structure in the residue. The pores are formed by the oxidation of layer segments of the graphite structure at high temperatures and in the presence of steam. Approximately 50% of the carbon is consumed in this step. The resulting activated carbon structure is highly porous, having a surface area of approximately $1000 \text{ m}^2/\text{g}$ (Weber, 1972). It is this large surface area that gives activated carbon its high adsorptive capacity.

While activated carbon is the most common adsorbent, a number of synthetic adsorbents have recently been developed. These adsorbents are made from various polymers, and usually take the form of spherical beads. Applications in water treatment have been limited, but in wastewater treatment synthetic adsorbents have proven to be suited for many industrial and municipal applications (van Vliet and Weber, 1981). Synthetic adsorbents tend to have a higher reversibility of adsorption than activated carbon, and so have potential for applications where by-product recovery may be attractive. Organic compounds that have been recovered effectively from waste streams using synthetic adsorbents include phenol, chlorinated phenols, aromatic and aliphatic nitro-compounds, and chlorinated pesticides (van Vliet and Weber, 1981).

2.3 Contacting Systems

The simplest adsorption contacting system is the completely mixed batch adsorber (Figure 2.1A). In this case the adsorbent is mixed with the influent and allowed to

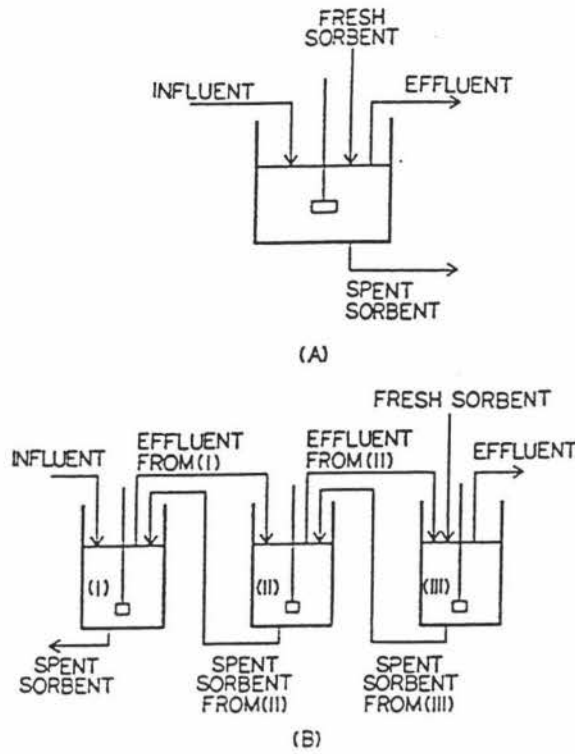


Figure 2.1: Batch Adsorption Configurations (Noll *et al*, 1992)

approach equilibrium, after which the two phases are separated for subsequent treatment or disposal. Unless the equilibrium capacity of the adsorbent is highly favourable, the batch configuration results in a low removal efficiency, as the adsorbent equilibrates with the low effluent contaminant concentration, resulting in a correspondingly low adsorbent loading.

The use of two or more batch adsorbers in series (Figure 2.1B) improves the efficiency of the process. Spent adsorbent is transferred to the preceding adsorber and is finally discarded after leaving the first adsorber in the series. This means that all of the discarded adsorbent has been in contact with the highly concentrated solution in the first adsorber, thus achieving maximum solute loading. Drawbacks of this configuration are the increased complexity of the system and the slow approach to equilibrium at the low solute concentrations of the last adsorbers. For

these reasons, batch adsorber configurations are seldom used unless other considerations such as pressure drop dictate otherwise.

The most efficient contacting system for adsorption processes is the fixed bed adsorber. This is because fresh influent is continually being passed over the adsorbent in the fixed bed, so that saturated adsorbent is in equilibrium with the maximum solution concentration and is therefore fully loaded. Fixed bed adsorbers also have the advantage of not requiring the separation of the adsorbent from the water after contact.

2.4 Adsorption in Fixed Beds

In fixed bed operation the portion of the bed close to the inlet is continuously contacted with the highly concentrated influent stream and so becomes fully loaded first. A concentration gradient of adsorbed solute develops in the adsorbent bed, from equilibrium near the inlet to zero downstream. The portion of the bed within the concentration gradient is the mass transfer zone (MTZ). It is within this zone that adsorption takes place.

As the saturated portion of the bed increases, the MTZ travels downstream and eventually exits the bed. This gives rise to a typical effluent concentration versus time profile, called the breakthrough curve (Figure 2.2). The breakthrough point is said to occur when the effluent concentration reaches the effluent quality limit. When the effluent concentration reaches the exhaustion concentration the bed is considered exhausted and is taken off line for adsorbent replacement.

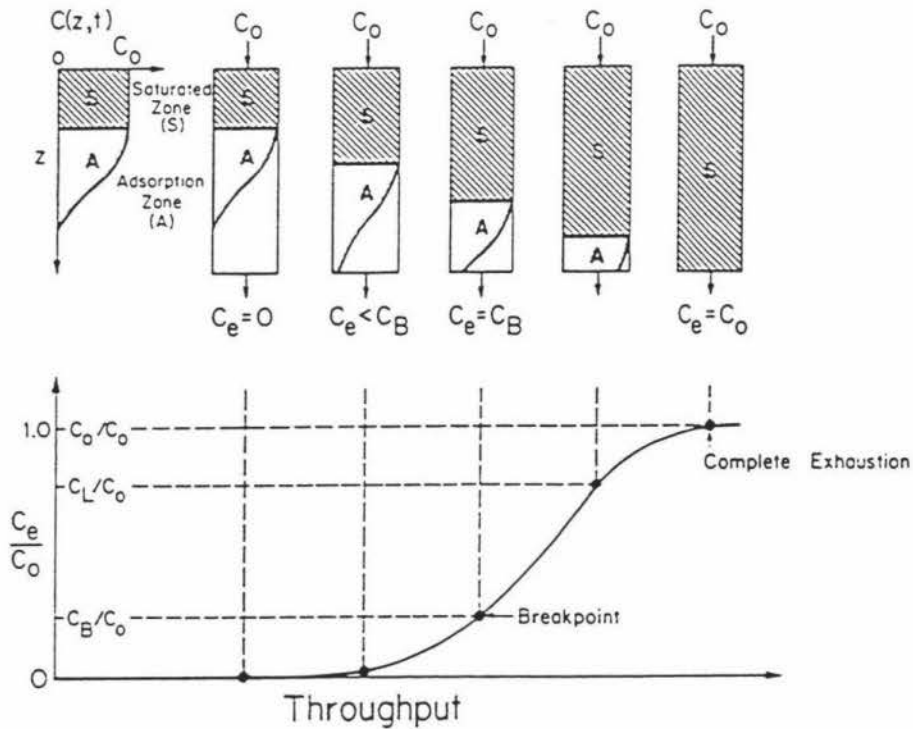


Figure 2.2: Breakthrough Curve for a Fixed Bed Adsorber (Weber, 1984)

There are several fixed bed configurations which can be used, the simplest being the single fixed bed adsorber. The drawback of this system is that when the breakthrough point is reached the adsorber must be taken off line for adsorbent regeneration. This is inefficient as at breakthrough an appreciable portion of the bed, has not been completely used. The length of bed not fully saturated at breakthrough is equal to the length of the mass transfer zone.

Using multiple fixed bed adsorbers in series improves the efficiency of the system, as when breakthrough occurs a fresh adsorber is connected to the end of the series. This allows adsorbers to become fully saturated while the MTZ is contained in downstream beds, thus maintaining effluent quality standards. When an adsorber becomes saturated it is taken off line for adsorbent replacement, after which it is connected to the end of the series.

Alternatively multiple adsorbers can be operated in parallel. Effluent from columns ready for regeneration is blended with effluent from fresh columns, allowing individual columns to be loaded to exhaustion while maintaining effluent quality.

The continuous moving bed system is an extension of the beds in series configuration. The adsorbent bed moves countercurrent to the wastewater as this means that adsorbent leaving the bed receives the maximum possible solute loading. Spent adsorbent is regenerated and returned to the top of the column. The moving bed system eliminates the need for standby equipment and reduces the level of adsorbent inventory required, but is expensive and so is used mainly in large installations (Noll *et al*, 1992).

2.5 Adsorption System Design

The first stage in the design of an adsorption system is the assessment of the feasibility and efficiency of the process. The equilibrium properties of an adsorbent/wastewater system determine the feasibility of the process by dictating the maximum amount of contaminant that can be loaded onto the adsorbent. The extent to which the adsorbent is loaded during operation determines the efficiency of the process. This is a function of the kinetic properties of the system, as well as the contaminant concentration and hydraulic conditions in the bed. As mentioned, for a fixed bed adsorber the unsaturated portion of the adsorbent at breakthrough is the mass transfer zone. Hence the efficiency of a fixed bed adsorption process largely depends on the shape and size of the MTZ, and the efficient design of a fixed bed adsorption system requires knowledge of the shape and size of the MTZ for the particular system under investigation.

Due to the complex nature of most wastewaters, the most reliable way to evaluate the size and shape of the MTZ is to conduct pilot column tests under similar conditions to those expected in the full-scale column. The bed depth service time method (Eckenfelder, 1980) is an example of this approach. Pilot columns are run in series, and the breakthrough curves of the columns plotted against cumulative time. From these curves the times taken for each column to reach breakthrough and exhaustion are determined and plotted against cumulative bed depth. This plot is the bed depth service time (BDST) curve (Figure 2.3). The BDST shows the

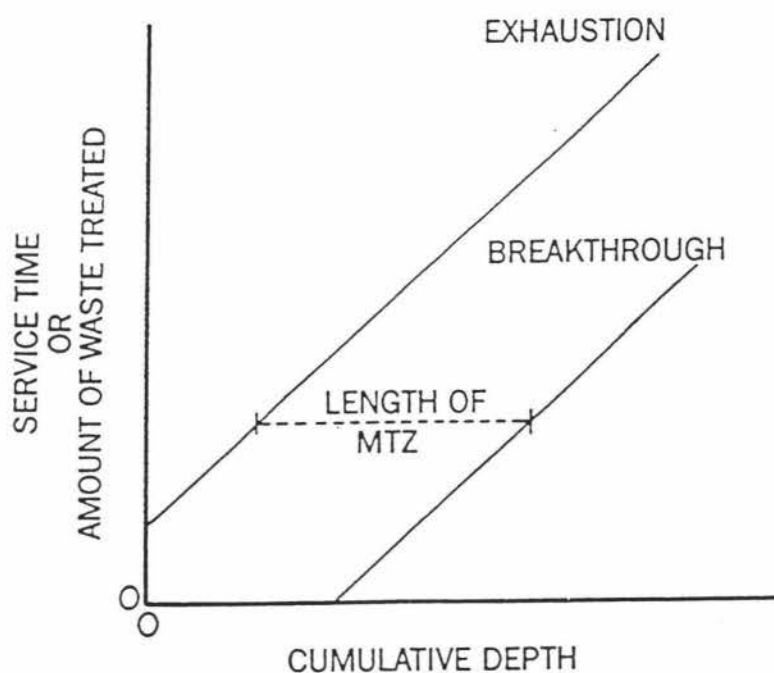


Figure 2.3: Bed Depth Service Time Curve for a Fixed Bed Adsorber
(Noll *et al.*, 1992)

relationship between service time or volume of water treated, and bed depth. The horizontal distance between the breakthrough and exhaustion lines is equal to the depth of the MTZ, while the inverse of the slope of the lines gives the velocity of the MTZ along the bed. The velocity of the MTZ multiplied by the cross-sectional area of the adsorber and the bulk density of the adsorbent is equal to the adsorbent usage

rate, which can be used to determine the required adsorbent regeneration capacity.

Given this information it is possible to determine the adsorber bed depth. For a continuous moving bed adsorption system the minimum bed depth to produce the desired contaminant removal is equal to the depth of the MTZ. A long MTZ would suggest that a multi-stage system was required in order to ensure adequate adsorbent utilisation. For a multi-stage system the depth of a single stage is related to the depth of the MTZ as follows:

$$d = \frac{D}{n-1} \quad (2.1)$$

(Eckenfelder, 1980)

where n = number of stages in series (not including one in standby)

D = depth of adsorption zone

d = depth of single stage

Selecting a large number of stages will result in a more complicated system but small bed size and low adsorbent inventory. A small number of stages will result in simpler operation but higher adsorbent inventory and larger plant size.

Although pilot studies are an important part of the design process, they are also costly and time-consuming. This means that it is often not possible to conduct all of the trials necessary in order to assess a system's performance under a wide range of conditions. A sub-optimal design may result. Mathematical models can aid the design process by providing a fast and reliable method of predicting fixed bed performance. Once verified on a pilot scale plant, the model can be used to predict

column performance under a wide range of conditions, thus helping to ensure that the design is an optimal one. The construction of an accurate model depends on an understanding of adsorption phenomena and a knowledge of the equilibrium and kinetic behaviour of the system being studied.

2.6 Adsorption Phenomena

Adsorption results from a variety of different types of attractive forces between solute molecules, solvent molecules and the molecules of an adsorbent. Accordingly, three categories of adsorption can be distinguished according to the class of attractive force which predominates: physical, chemical and electrostatic (Weber, 1972).

Physical adsorption occurs due to the interaction of the dipole moments of the adsorbent and solute molecules. The dipole moments may be permanent, in the case of polar molecules, or induced by nearby polar molecules or ions. These forces, which include the Debye, Keesom and London dispersion forces, are generally weak and act over short ranges, the associated energy decreasing inversely with the sixth power of the distance separating the molecules (Israelachvili, 1985). The forces that act in chemical adsorption are also short range but are of high energy, having all of the characteristics of covalent bonds (Weber, 1993). Electrostatic forces occur where discretely charged molecules are involved and act over longer ranges than physical and chemical forces.

In reality, the classes of forces described above do not act separately and it is their combined effect that determines the net driving force in an adsorption system. The

net driving force may be predominantly "adsorbent-motivated", caused by the affinity of the solute for the adsorbent, or it may be "solvent-motivated", driven by the lack of affinity of the solute for the solvent, as occurs with hydrophobic contaminants in aqueous solutions (Weber, 1972).

2.7 Equilibrium Isotherm Models

Models for characterising the equilibrium distribution of a solute between the solvent and the adsorbent phases typically relate the amount of solute, q_e , adsorbed per unit mass of adsorbent to the amount of solute, C_e , retained in the solvent phase. An expression of this type, evaluated at a fixed system temperature, constitutes what is known as an adsorption isotherm. Examples of the general types of isotherm are illustrated in Figure 2.4.

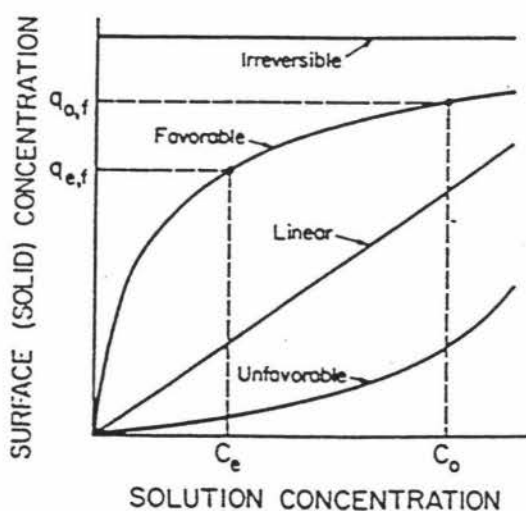


Figure 2.4: Types of Adsorption Equilibrium Isotherms (Weber, 1972)

Various models have been developed to describe observed adsorption isotherms. The simplest model is the linear isotherm:

$$q_e = K_D C_e \quad (2.2)$$

K_D is often referred to as the distribution or partition coefficient. The linear isotherm has been found to adequately describe adsorption in certain systems, usually at very low solute concentrations and for adsorbents of low adsorption capacity (Weber, 1993).

The Langmuir isotherm was developed on the assumption that the energy of adsorption is the same for each molecule and independent of surface coverage, and that adsorption involves no interactions between adsorbed molecules and leads to the deposition of a single layer of solute molecules on the surface of the adsorbent. Given these assumptions, the Langmuir model can be derived from either kinetic or thermodynamic approaches. The resulting expression is:

$$q_e = \frac{Q b C_e}{1 + b C_e} \quad (2.3)$$

The parameter Q represents the adsorbed solute concentration corresponding to complete monolayer coverage, while b is a coefficient related to the enthalpy of adsorption.

The Freundlich isotherm is the most widely used adsorption isotherm model in water and wastewater treatment applications. Although it is mostly an empirical

relationship, it has been shown to have a thermodynamically rigorous basis for adsorption on heterogeneous surfaces (Adamson, 1967). This model has the general form:

$$q_e = K C_e^{1/n} \quad (2.4)$$

The parameter K relates to adsorption capacity, being equal to the capacity of the adsorbent in equilibrium with a solution concentration of 1 mg/L. A high value of $1/n$ (steep slope) indicates high adsorption capacity at strong solute concentrations and poor adsorption at dilute concentrations. A low value of $1/n$ indicates high adsorption capacity throughout the concentration range.

2.8 Equilibrium Studies

Breakthrough profiles generated from predictive dynamic models are particularly sensitive to equilibrium parameters (Weber and Smith, 1987). It is thus important in the formulation of a modelling approach to select an equilibrium model that can accurately describe isotherm data. Many studies have been conducted on the equilibrium adsorption capacity of activated carbon for various organic pollutants. As mentioned earlier, the most common isotherm model used to fit equilibrium data is the Freundlich isotherm. For example, Speth and Miltner (1990) presented Freundlich isotherms for 58 compounds in distilled-deionized water, filtered river water and filtered groundwater. Urano et al (1991) studied the adsorption capacities and rates of seven chlorinated organic compounds for six commercial GAC's. All isotherms were expressed by the Freundlich equation.

Sorial et al (1993) Studied the impact of GAC characteristics on adsorption capacity for p-chlorophenol. Isotherms were collected under anoxic and oxic conditions to evaluate the potential for polymerisation of phenolic compounds on the surface of the GAC. The study revealed that the characteristics of GAC have a direct impact on the adsorption capacity and on the potential for surface catalysed polymerisation reactions. Van Vliet and Weber (1981) compared the adsorption equilibria of p-toluenesulfonate and p-chlorophenol on two activated carbons and eight synthetic adsorbents. At low concentration ranges, the activated carbons showed considerably higher capacities than the synthetic adsorbents. At higher concentration levels, the capacities of the adsorbents tended to converge.

Ying et al (1990) measured the adsorptive capacities for a variety of major organic constituents of wastewaters, in both pure water and actual wastewater samples. The capacity reduction for most wastewater constituents could be correlated with the amount of total organic carbon (TOC) attributable to the target compound. Smith *et al* (1987) also studied the impact of background dissolved organic matter (DOM) on the adsorption of a target organic compound (lindane). Increasing background DOM concentrations were found to decrease the K value of lindane isotherm, while the slope remained essentially unchanged.

2.9 Adsorption Kinetics

Many different kinetic models for the description of adsorption by porous adsorbents have been developed, based on various combinations of mass transfer resistances. The most successful models are of a dual resistance nature, describing the transport of the solute molecule across the stagnant liquid film surrounding the adsorbent

particle, followed by transport within the pore structure of the adsorbent. Variations of such models are distinguished by the means of expressing the intraparticle mass transport step. Figure 2.5 shows a schematic view of the various mass transfer steps involved in the adsorption process.

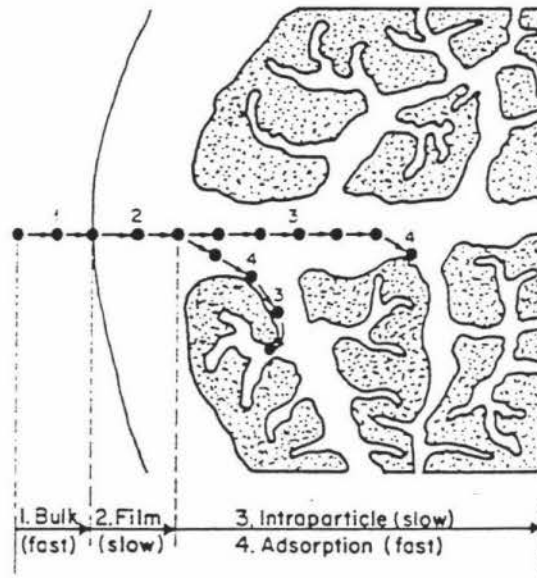


Figure 2.5: Transport Steps in Adsorption by Porous Adsorbents (Weber, 1984)

2.9.1 Intraparticle Transport

The simplest way of describing transport within the adsorbent particle is the linear driving force approximation (Bhaskar and Bhamidimarri, 1991, Peel and Benedek, 1981). Adsorption is assumed to occur on the outer surface of the particle, and mass transfer into the particle occurs as a result of the difference in concentration between the surface and the interior. A uniform solid phase concentration is assumed, represented by the average solute concentration in the particle. The intraparticle

mass transfer equation can be described as:

$$\frac{d\bar{q}}{dt} = \frac{k_p A}{V} (q_s - \bar{q}) \quad (2.5)$$

Where k_p is the intraparticle mass transfer coefficient and q is the average solute concentration inside the particle.

A quadratic driving force expression was found to give better results than the simple linear driving force expression (Peel and Benedek, 1981). The quadratic driving force expression can be written:

$$\frac{d\bar{q}}{dt} = \frac{k_p A}{V} \left(\frac{q_s^2 - \bar{q}^2}{2\bar{q}} \right) \quad (2.6)$$

A more descriptive analysis of intraparticle diffusion is given by the pore transport model (Weber and Chakravorti, 1974, Westermarck, 1975). This model pictures the adsorbent particles as consisting of a solid phase interspersed with small pores. Solute molecules reach internal adsorption sites by diffusing through the pore liquid. Solute concentration in the pore liquid is a function of radial position and solid-phase concentration is assumed to be at equilibrium with the adjacent pore liquid. The transport of solute within the internal pores can be described by:

$$\rho_p \frac{\partial q}{\partial t} + \epsilon \frac{\partial C_r}{\partial t} = \epsilon \frac{D_p}{r^2} \frac{\partial}{\partial r} \left(r^2 \frac{\partial C_r}{\partial r} \right) \quad (2.7)$$

Where C_r is the solute concentration in the internal pore liquid and D_p is the internal

pore diffusion coefficient. The terms on the left hand side represent solute buildup in the solid and liquid phases of the particle respectively, while the right hand side represents diffusion of solute into the pores.

An alternative to the pore diffusion model which has been widely used is the homogeneous surface diffusion model (HSDM) (Weber and Chakravorti, 1974, Crittendon and Weber, 1978). In this model, adsorption occurs only at the outer surface of the particle. The solute molecules penetrate further into the particle by creeping along the pore surfaces. The driving force for this movement is the concentration gradient of solute within the particle, which is pictured as a homogeneous sphere but with a surface diffusion coefficient which takes into account the internal porosity of the actual particles. Intraparticle transport can hence be described by:

$$\frac{\partial q}{\partial t} = \frac{D_s}{r^2} \frac{\partial}{\partial r} \left(r^2 \frac{\partial q}{\partial r} \right) \quad (2.8)$$

Where D_s is the surface diffusion coefficient.

The homogeneous surface diffusion model has been successfully applied to many adsorption systems, however the model was found to be inaccurate in systems where there is a rapid uptake of solute followed by a slow approach to equilibrium. For instance, Peel and Benedek (1980) conducted isotherm studies with phenol and o-chlorophenol and found that up to 80% of adsorption capacity was taken up within the first few hours, but the remaining capacity was utilized very slowly. A modification of the homogeneous surface diffusion model which better describes this

slow approach to equilibrium is the dual pore-diffusion model (DPDM) (Peel *et al*, 1981). This model envisages the particle structure as consisting of relatively large macropores and smaller micropores which hinder solute diffusion into the particle. The resulting kinetic model involves two in-series intra-particle mass transport steps: macropore surface diffusion followed by a micropore transport step. The micropores are assumed to be homogeneously distributed throughout the particle and to branch off the macropore network, which is responsible for radial transport. Slightly differing versions of the DPDM are presented by Weber and Liang (1983) and Famularo *et al* (1980).

2.9.2 Kinetic Parameter Estimation

Solution of the HSDM for fixed-bed systems requires the determination of the two mass transfer resistance parameters: the film diffusion coefficient, k_f , and the surface diffusion coefficient, D_s . Traditionally this has been achieved by fitting the HSDM to batch adsorber data in order to find the parameter values that best fit the model to the experimental data. In order to simplify this process, Hand *et al* (1983) were able to experimentally eliminate k_f by achieving sufficiently high agitation, then determine D_s by applying the HSDM to the batch data. Peel *et al* (1981) and Bhaskar and Bhamidimarri (1992) calculated k_f using the initial portion of the batch adsorber data, when film transfer is assumed to dominate the overall mass transfer rate. The surface diffusion coefficient was calculated by fitting the model to the entire data. Crittendon and Weber (1978), Traegner and Suidan (1989) and Roy *et al* (1993) proposed mathematical dual parameter search techniques where both parameters were solved simultaneously.

One disadvantage of using batch adsorber methods to determine mass transfer parameters is that hydrodynamic conditions in a batch adsorber are different from a fixed-bed column, so that the fixed-bed film transfer coefficient must be estimated from empirical correlations (Crittendon and Weber, 1978). Roberts *et al* (1985) compared predicted k_f values from four mass transfer correlations with values obtained by fitting the HSDM to column data, and found that Gnielinski's correlation gave the most accurate prediction.

In order to avoid using correlations to determine column k_f values, Liu and Weber (1981) proposed a method to simultaneously determine both external film and intra-particle diffusion coefficients using a short column where solute breakthrough occurs immediately. The method provided parameters that accurately simulated experimental breakthrough profiles. Other researchers have used this technique to model fixed-bed systems (Fettig and Sontheimer, 1987, Smith *et al*, 1987).

2.10 Modelling Fixed Bed Adsorbers

Most of the kinetic studies mentioned in the previous section also included bench-scale column experiments to assess the ability of the kinetic model to predict experimental breakthrough curves. Model predictions are achieved by conducting solute mass balances for the solid and liquid phases. Figure 2.6 shows an overview of this approach. Using this technique, the HSDM has shown to be an effective model for predicting the experimental breakthrough curves of many single-solute systems.

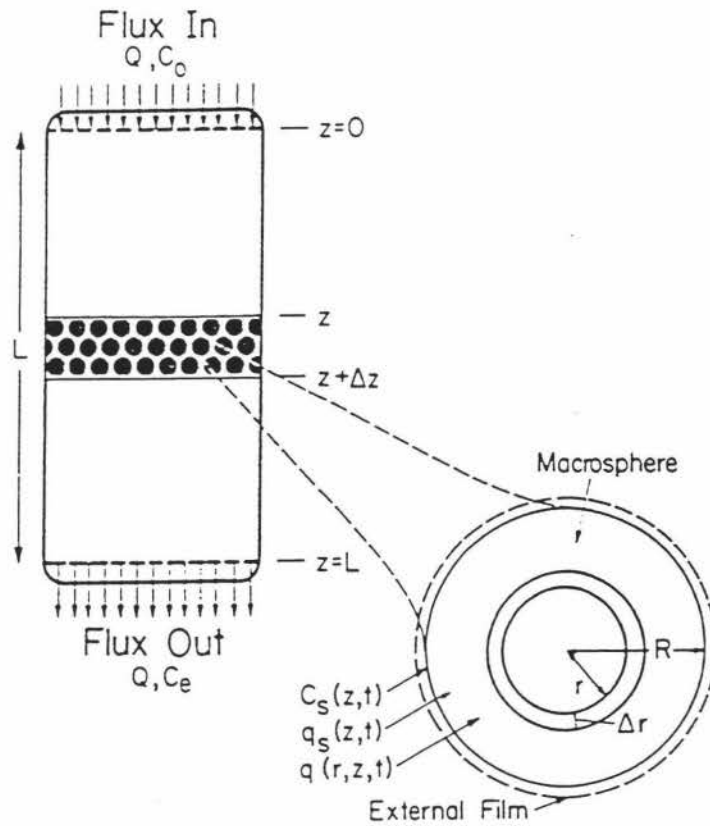


Figure 2.6: Material Balances in a Fixed Bed Adsorber (Weber, 1984)

A method of determining the breakthrough curves of large scale adsorbers from bench scale columns was presented by Smith *et al* (1986) and Crittendon *et al* (1991). Scaling equations were derived from dimensionless groups found in the HSDM. The choice of carbon particle size determined the appropriate hydraulic loading rate and empty bed contact time (EBCT) of the small column in order to simulate the full scale column. The method does not require the use of numerical models, assesses both adsorption capacity and kinetics and has low operating and capital costs.

The bottom line for adsorption modelling is whether and how well it can facilitate the engineering design of actual systems. Models which are based on known adsorption phenomena and which use experimentally determined equilibrium and kinetic parameters have proved to be useful in simulating bench-scale data and designing appropriate pilot programs. In particular the homogeneous surface

diffusion model has been successfully applied to many single-solute systems involving various adsorbents and wastewaters (Weber and Smith, 1987). It is for this reason that the HSDM was selected for this study.

3. MATERIALS AND METHODS

3.1 Carbon

The activated carbon used for this study was manufactured by Calgon Corp (Pittsburgh, PA). The carbon was sieved and the 0.60 - 0.85 mm fraction was retained for use. The carbon was washed with distilled water for an hour to remove fines, then dried at 105 degrees C overnight and stored in a desiccator until used.

3.2 Chemicals

PCP used was manufactured by Sigma Chemical Company (St Louis, Mo). Concentrated stock solutions were made by dissolving the PCP powder in NaOH solution. Subsequent concentrations for experiments were obtained by diluting the stock solution with distilled water.

3.3 PCP Analysis

In the equilibrium experiments PCP concentration was measured using a UV spectrophotometer (Shimadzu UV-1201, 308 nm wavelength). A calibration curve for this analysis is shown in Appendix 1. In order to minimise the amount of solution removed from the reactor during the kinetics experiments, samples were analysed using an HPLC (Waters 600E solvent delivery system, mobile phase 90% methanol, 9.9% water, 0.1% acetic acid; Waters 486 absorbance detector, wavelength 308 nm). This device only required a 0.6 ml sample.

3.4 Equilibrium Studies

Equilibrium isotherms were obtained by mixing 100 ml of PCP solution with varying masses of activated carbon in 250 ml flasks. Usually 12 flasks were used for each isotherm experiment. The flasks were sealed with aluminium foil and placed in a thermostatic orbital shaker (Gallenkamp orbital incubator) and left for 24 hours to equilibrate. Samples from the flasks were filtered through a 0.45 micron filter (Millipore) and analyzed as described above. The pH of each flask was also measured using a pH meter (Orion model 230A).

3.5 Batch Kinetics Experiments

The kinetic experiments were conducted in a baffled 5 litre reactor (Figure 3.1). The

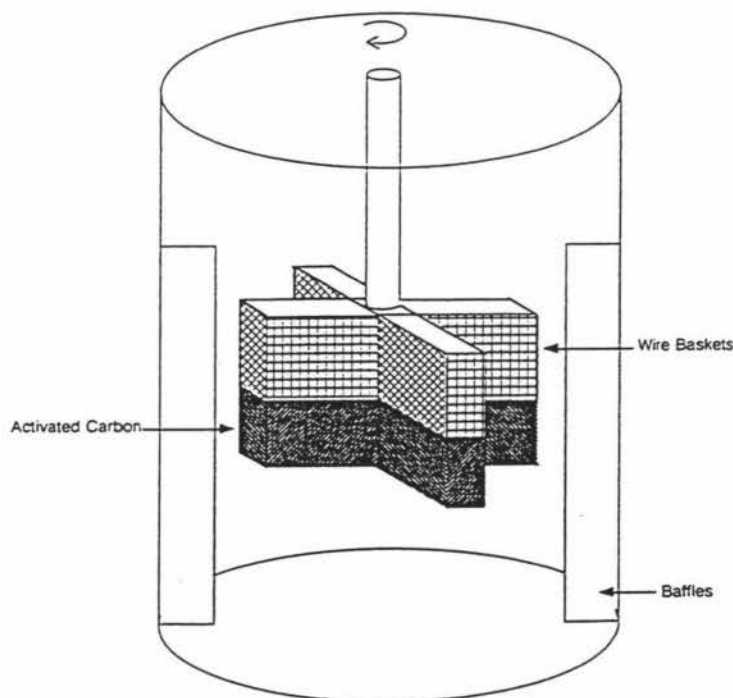


Figure 3.1: Rotating Wire Basket Adsorption Batch Reactor

weighed activated carbon was placed in wire mesh baskets (US standard 40 mesh). The reactor was filled with 3 litres of 250 mg/L PCP solution, and the baskets were rotated inside the reactor by a variable speed stirrer motor (Janke and Kunkel RW20). 0.6 ml samples were taken by pipette, and analyzed using an HPLC as described above. Using the HPLC kept the volume change in the reactor during the experiment down to a minimum. For the first two minutes samples were taken every ten seconds in order to calculate the initial slope of the concentration versus time graph. Following that, samples were taken every ten minutes for the first hour, then hourly for seven hours.

3.6 Column Studies

The experimental setup for the column experiments is shown in Figure 3.2.

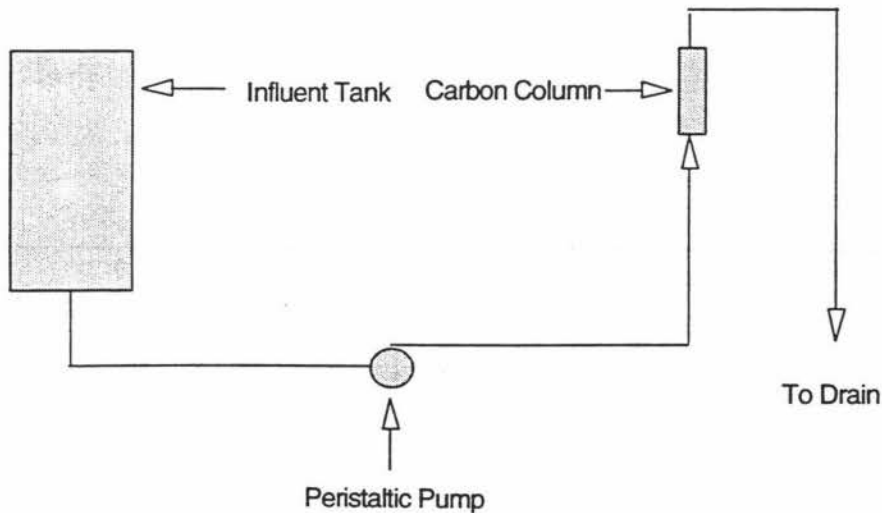


Figure 3.2: Experimental Setup for Column Experiments

All column experiments were conducted using a 63 mm long perspex column with a 10 mm inside diameter. Prior to all experiments the column was washed with distilled water overnight to remove any carbon fines. PCP solution was held in a 10 litre glass reservoir and introduced to the column in an upflow configuration via a peristaltic pump (masterflex model no. 7553-85, pump head masterflex model no. 7016). Flow rates ranged from 2.8 to 6.2 ml/minute. Column temperature was maintained via a water jacket connected to a thermostatic water circulator (Julabo HTC). All effluent and influent concentrations were measured using a UV spectrophotometer (same as for the equilibrium experiments).

4. EQUILIBRIUM STUDIES

4.1 Preliminary Studies

The contact time between the activated carbon and the solution being studied is an important parameter in achieving accurate isotherm data (Peel and Benedek, 1980). In order to determine the time necessary to achieve equilibrium, an equilibrium time test was carried out. Equal amounts of carbon (1 g) were placed in 250 ml flasks containing 100 ml of 25 ppm PCP solution, which were placed in an orbital shaker at 25 C. One flask was taken out of the shaker every hour and analysed for PCP concentration. The results are shown in figure 4.1. As can be seen, after three hours

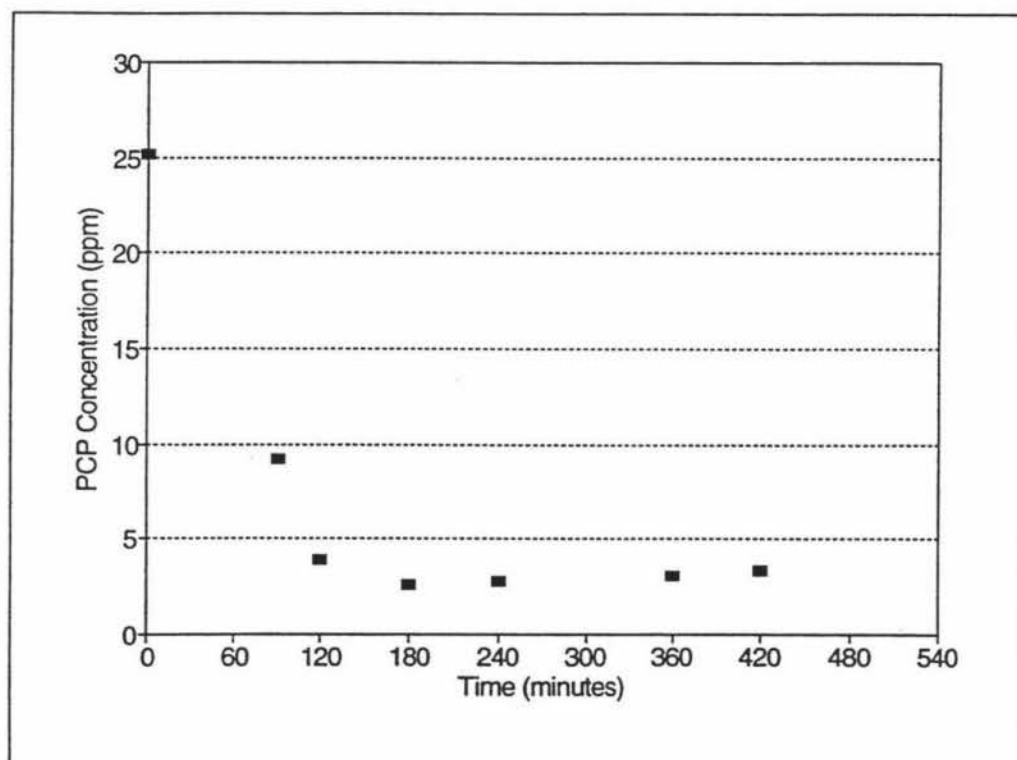


Figure 4.1: Equilibrium Time Test

the solution concentration is constant, indicating equilibrium was attained after approximately three hours. To be on the safe side, all equilibrium experiments were conducted using a contact time of 24 hours. Evaporation losses were prevented by sealing the flasks.

4.2 Equilibrium Isotherms

Isotherms were carried out at two initial concentrations, 250 ppm and 500 ppm. Typically 12 points were calculated in each isotherm experiment. The isotherms were repeated to verify accuracy. The results of one of the 500 ppm isotherms were checked using an HPLC and were found to agree well with the uv spectrophotometer results. The raw data was found to best fit the Freundlich equation, an observation that has been found in most activated carbon studies. Figures 4.2 and 4.3 show the 250 ppm and 500 ppm isotherms, and Figures 4.4 to 4.6 show the respective 250 ppm, 500 ppm and combined log-log plots.

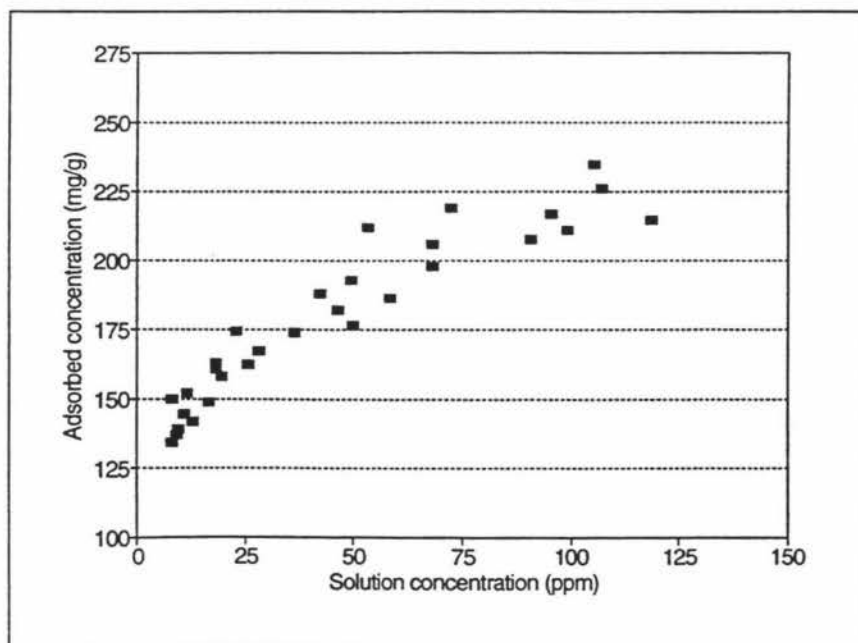


Figure 4.2: Equilibrium Isotherm, Initial PCP Conc. = 250 ppm

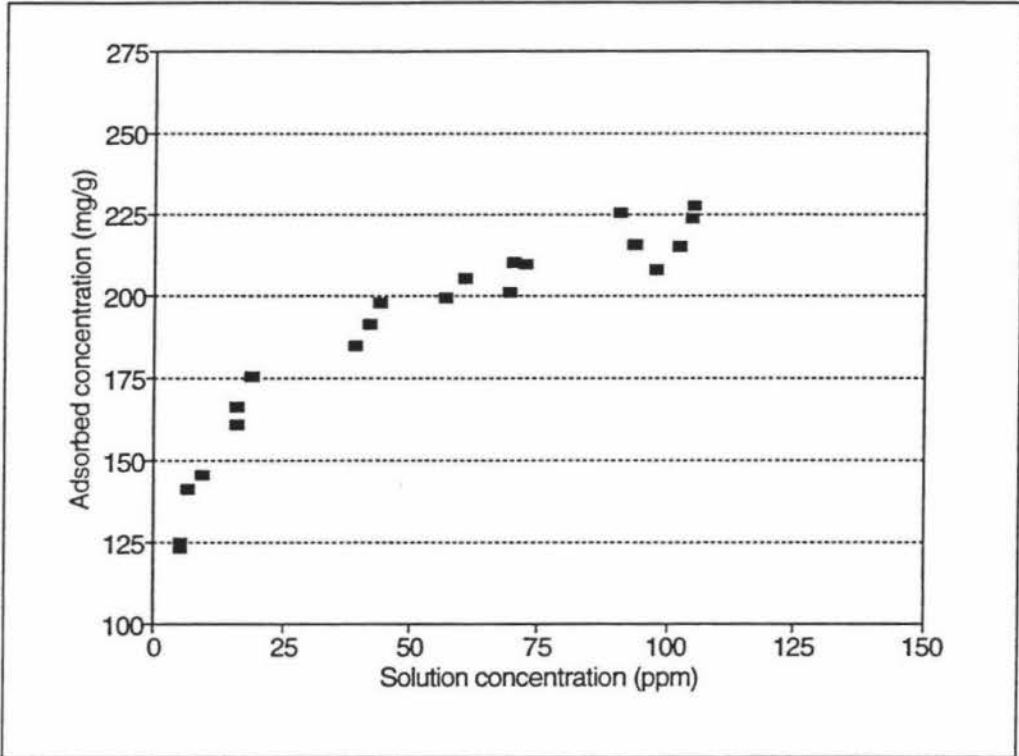


Figure 4.3: Equilibrium Isotherm, Initial PCP Conc. = 500 ppm

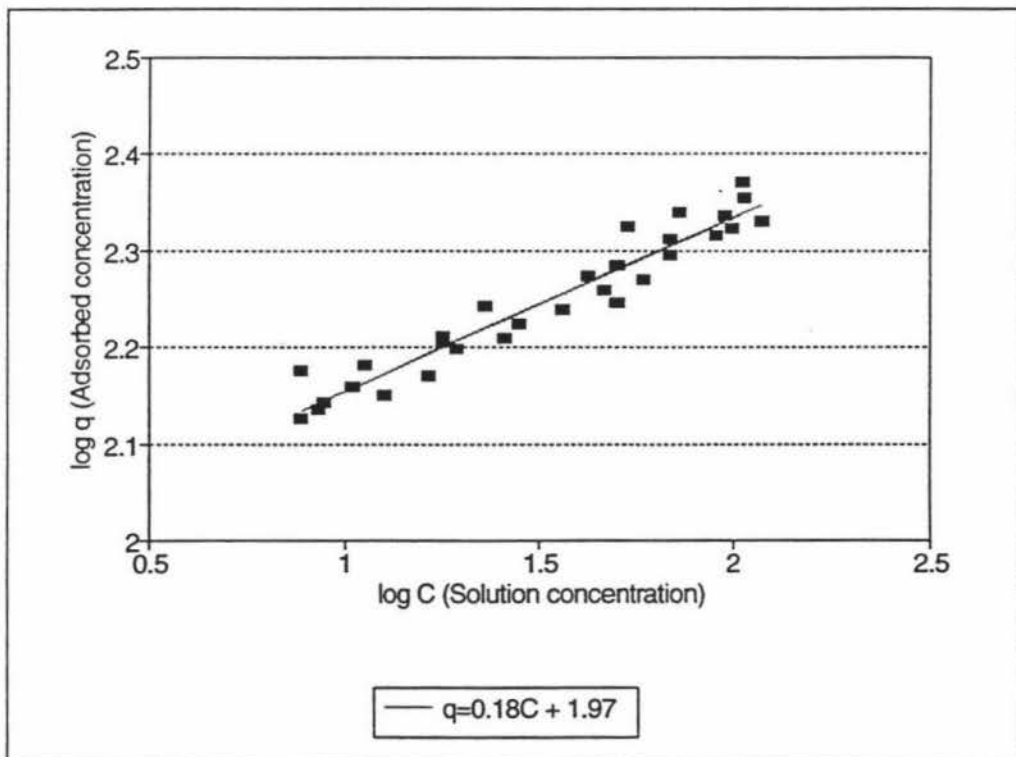


Figure 4.4: Equilibrium Isotherm, Initial PCP Conc. = 250 ppm

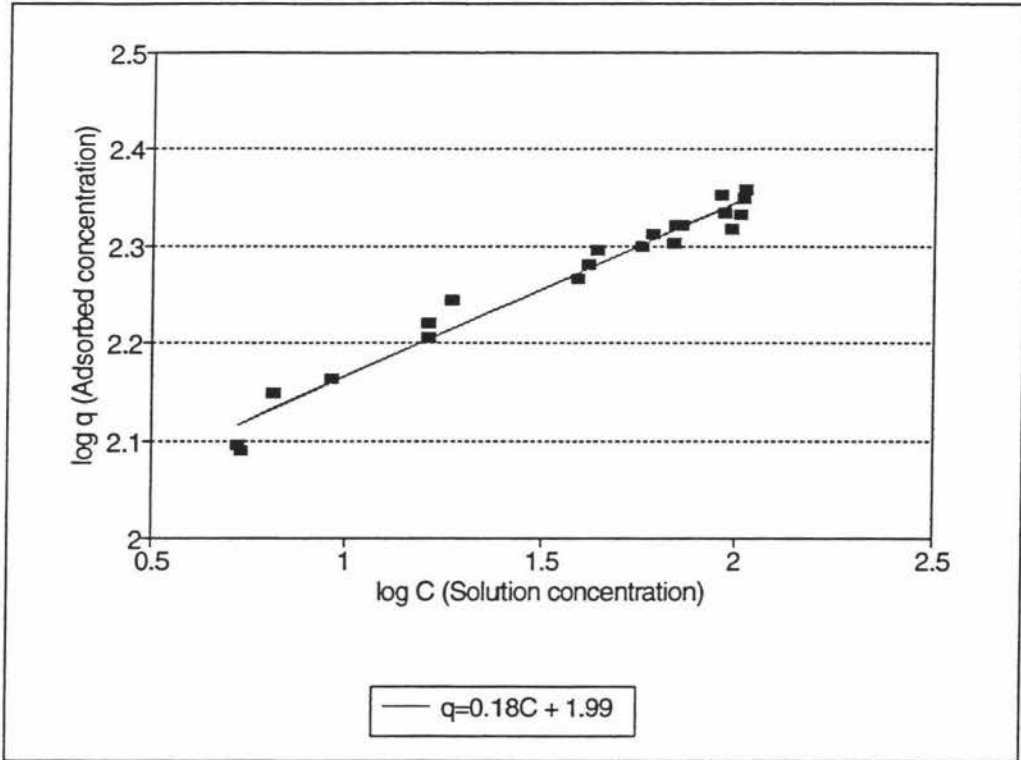


Figure 4.5: Equilibrium Isotherm, Initial PCP Conc. = 500 ppm

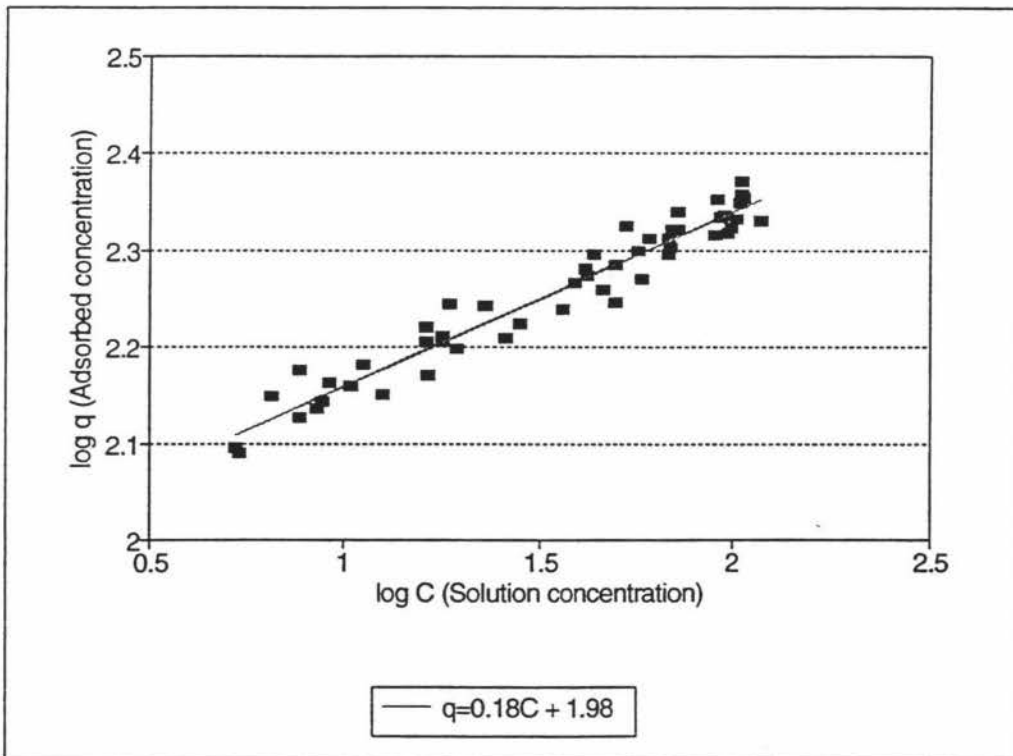


Figure 4.6: Equilibrium Isotherm, Initial PCP Conc. = 500 ppm and 250 ppm

Table 4.1 shows the Freundlich coefficients corresponding to Figures 4.4 to 4.6.

Table 4.1: Freundlich Isotherm Coefficients

Isotherm:	No. of Points:	K	95% error bounds:	1/n	95% error bounds:
250 ppm	30	94.3	1.1	0.180	.019
500 ppm	22	97.0	1.1	0.179	.014
Combined	52	95.0	1.1	0.180	.013

There is very little difference between the 250 and 500 ppm isotherms, suggesting that the Freundlich isotherm is an appropriate choice over this concentration range.

The Freundlich isotherm, while basically an empirical relationship, gives an indication of the adsorptive capacity of the system. The constant K is an indicator of adsorption capacity, being equal to the capacity of the activated carbon in mg/g in equilibrium with a solution concentration of 1 mg/l. The slope 1/n reflects the sensitivity of the adsorptive capacity to changes in contaminant concentration. The adsorption isotherm can hence provide the basis for determining whether the system is suitable for carbon adsorption treatment, as well as providing a preliminary estimate of carbon usage, and predicting the changes in adsorptive capacity if contaminant concentrations change.

For comparison of the results with the coefficients of similar compounds, Table 4.2 shows the Freundlich constants for some similar organic compounds found in the

literature.

Table 4.2: Freundlich Coefficients for Phenolic Compounds in Water

Author	Compound	K	1/n
Sorial <i>et al</i> (1993)	P-chlorophenol	117	0.158
Weber & Liang (1983)	Phenol	46.7	0.310
	P-chlorophenol	111	0.176
	P-bromophenol	279	0.117
	P-nitrophenol	191	0.136

Table 4.2 shows that the substituted phenolic compounds are more easily adsorbable (as indicated by the K values) than phenol. The 1/n values indicate that the decrease in adsorptive capacity due to low solution concentrations is less for the substituted compounds than for phenol. These two observations indicate that the substituted phenolics are more suitable for carbon adsorption treatment than phenol.

The Freundlich constants obtained for PCP are of a similar order of magnitude to those of the substituted phenolics above, although the K value is slightly lower. The Freundlich constants obtained for PCP are similar to those of p-chlorophenol shown above, which is expected as they have a similar molecular structure, with PCP having five chlorine atoms attached to the phenol ring as opposed to one for p-chlorophenol.

5. ADSORPTION KINETICS

5.1. Homogeneous Surface Diffusion Model (HSDM)

The homogeneous surface diffusion model (HSDM) has been used in many studies to describe the adsorption of contaminants onto activated carbon in both completely mixed batch reactors (CMBR's) and fixed-bed systems (Weber and Smith, 1987). The object of the kinetics study was to apply the HSDM to a CMBR experiment in order to determine the kinetic coefficients necessary to predict fixed bed performance.

The schematic diagram of an activated carbon particle, given in Figure 5.1, illustrates the mechanisms of mass transport into the particle, as represented in the HSDM.

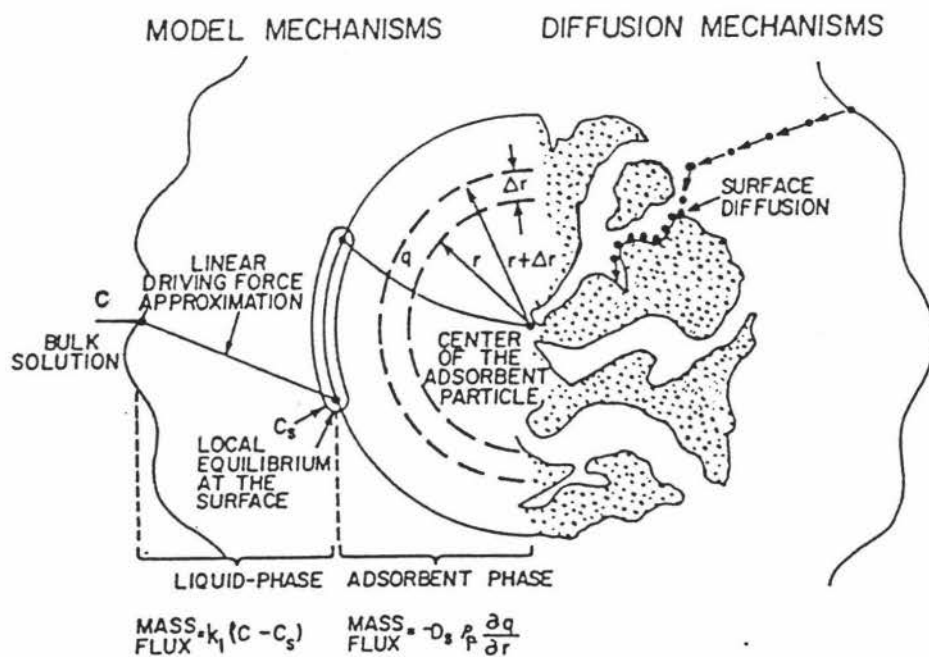


Figure 5.1: Mechanisms and Assumptions Incorporated in the HSDM

(Adapted from Hand, 1983)

The particle is surrounded by a stagnant liquid film, across which there is a linear concentration gradient of solute. At the particle surface, instantaneous equilibrium is assumed to occur between the liquid and adsorbed phases. Once adsorbed, solute molecules diffuse from the surface into the particle along the inner pore surfaces. Since the pore structure is very intricate, in the model the particle is represented as a solid sphere, with an effective diffusion coefficient taking into account the effect of the actual pore structure. Diffusion into the sphere is described by Fick's law.

5.2 Model Equations

The overall mass balance for the completely mixed batch reactor is:

$$V \frac{dC}{dt} = k_f A (C - C_s) \quad (5.1)$$

Where k_f is the film transfer coefficient, C_s is the solute concentration adjacent to the particle surface and A is the total adsorbent surface area (assuming spherical particles of radius R).

The mass balance for a carbon particle is:

$$\frac{\partial q}{\partial t} = \frac{D_s}{r^2} \frac{\partial}{\partial r} \left(r^2 \frac{\partial q}{\partial r} \right) \quad (5.2)$$

where D_s is the surface diffusion coefficient. The variable r denotes radial position within the particle, the origin being the centre of the particle.

The boundary conditions for the above equations are:

At the particle surface ($r = R$):

$$\frac{\partial q}{\partial r} = \frac{k_l}{\rho_p D_s} (C - C_s) \quad (5.3)$$

$$q_s = KC_s^{1/n} \quad (5.4)$$

Equation (5.3) ensures that the flux of solute diffusing into the particle equals the flux of solute across the stagnant film to the particle surface. Equation (5.4) ensures that the adsorbed solute at the particle surface is in equilibrium with the dissolved solute.

At the particle centre ($r = 0$):

$$\frac{\partial q}{\partial r} = 0 \quad (5.5)$$

(This ensures no solute diffusion across the particle centre).

At $t = 0$:

$$q = 0 \quad (5.6)$$

(Initially there is no adsorbed solute).

In order to solve equations (5.1) and (5.2), it is convenient to convert the variables into dimensionless form using the following definitions:

$$C^* = \frac{C}{C_o} ; q^* = \frac{q}{q_o} ; r^* = \frac{r}{R} ; \tau = \frac{D_s t}{R^2} \quad (5.7)$$

$$Bi = \frac{(k_l A / V)}{(D_s / R^2)} ; F = \frac{V C_o}{W q_o} \quad (5.8)$$

Where Bi is the Biot number, and represents the ratio of mass transfer across the liquid film to the rate of intraparticle diffusion. F is the solute separation factor, and W is the total weight of adsorbent. Given the above definitions, equations (5.1) to (5.6) can be rewritten:

$$\frac{dC^*}{d\tau} = Bi(C^* - C_s^*) \quad (5.9)$$

$$\frac{\partial q^*}{\partial \tau} = \frac{1}{r^{*2}} \frac{\partial}{\partial r^*} (r^{*2} \frac{\partial q^*}{\partial r^*}) \quad (5.10)$$

At $r^* = 1$:

$$\frac{\partial q^*}{\partial r^*} = \frac{BiF}{3} (C^* - C_s^*) \quad (5.11)$$

$$q_s^* = C_s^{*1/n} \quad (5.12)$$

At $r^* = 0$:

$$\frac{\partial q^*}{\partial r^*} = 0 \quad (5.13)$$

At $\tau = 0$:

$$q^* = 0 ; C^* = 1 \quad (5.14)$$

The dimensionless equations (5.9) to (5.14) above were solved numerically using a computer program which utilised a combination of orthogonal collocation, fourth order Runge-Kutte and Newton-Raphson techniques.

5.3 Results and Discussion

All kinetics experiments were conducted in a baffled reactor, with a liquid volume of 3 litres, as described in Section 3.4. Four experiments were carried out at varying stirrer speeds. The initial PCP concentration in each experiment was 250 mg/L. Figure 5.2 shows the plots of PCP concentration versus time for the four experiments.

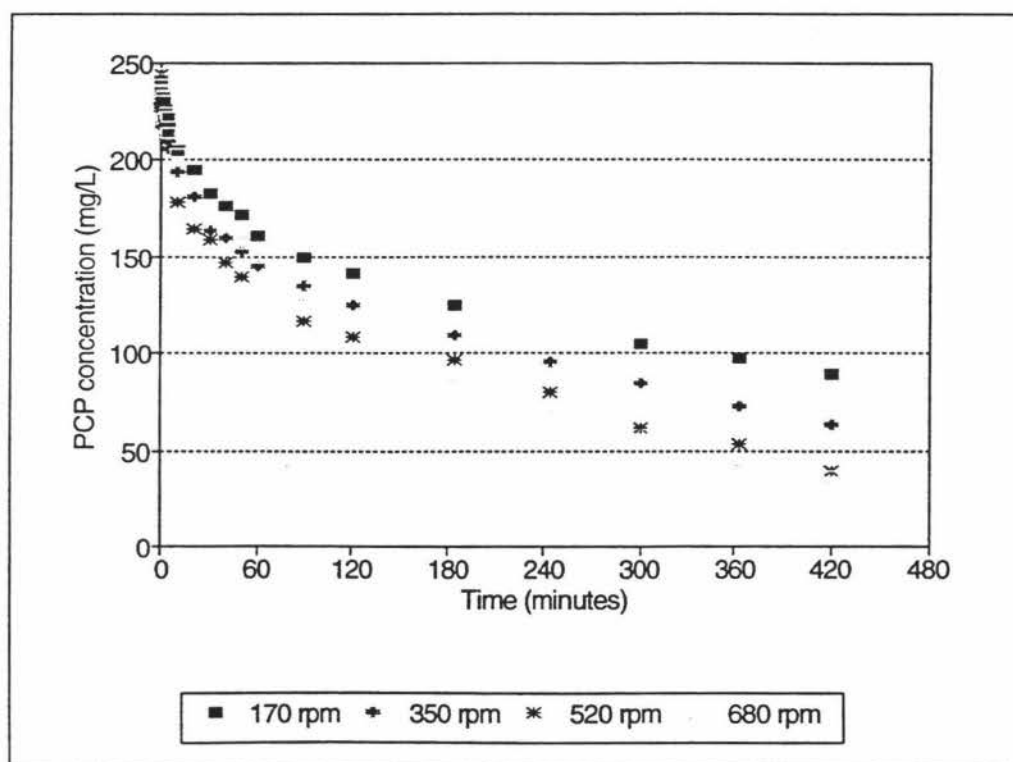


Figure 5.2: Solute Uptake Curves for Various Stirrer Speeds

5.3.1 Film Transfer Coefficients

The film transfer coefficient, k_f , was determined from the first few seconds of the solute uptake data, when intraparticle diffusional resistance can be assumed to be negligible (Peel *et al*, 1981; Bhaskar and Bhamidimarri, 1992). In this case the film transfer coefficient is proportional to the slope of a log (concentration) versus time graph. Figures 5.3 to 5.6 show these initial uptake plots for the four different stirrer speeds.

When the baskets were lowered into the reactor rapid initial adsorption of solute occurred. Part of this rapid uptake occurred in the brief delay before the stirrer motor was switched on. This explains the discrepancy between the initial points (taken before the baskets were lowered into the reactor) and the rest of the points in the initial uptake plots. For this reason the initial solution concentration points were not included in the initial slope calculations.

As expected, the initial slopes and k_f values increased with increasing stirrer speed (Table 5.1).

Table 5.1: Film Diffusion Coefficients Calculated From Initial Slope Data:

Experiment	Stirrer Speed (rpm)	Initial Slope = $k_f A/V$ (s^{-1})	$k_f \times 10^3$ (cm/s)
1	180	.00052	3.84
2	390	.00077	5.63
3	560	.00082	6.02
4	760	.00174	12.76

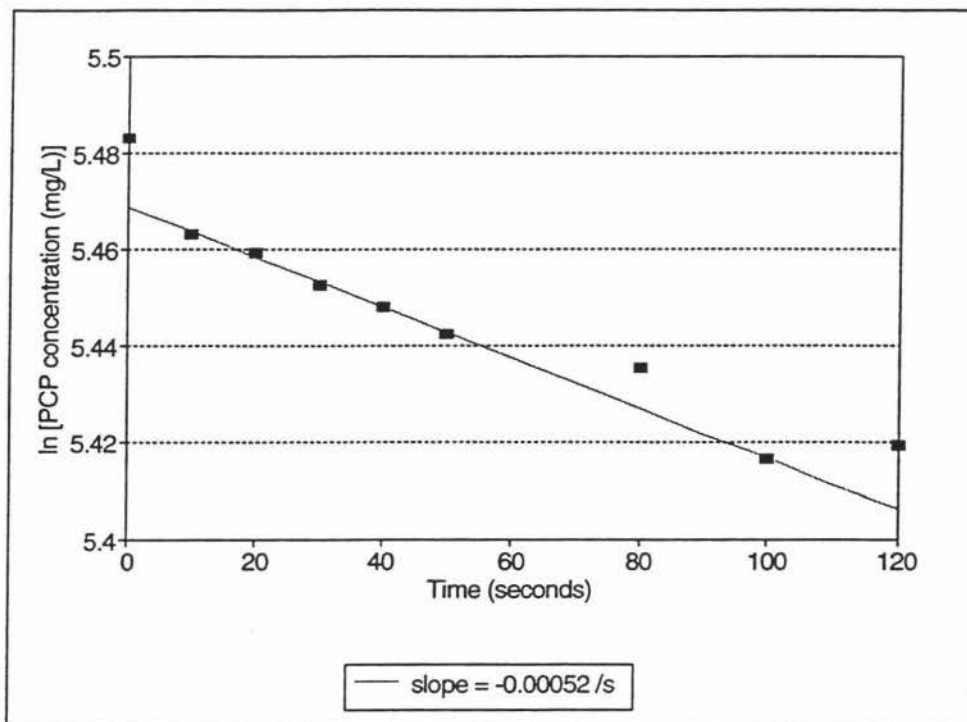


Figure 5.3: Initial Solute Uptake Plot for Stirrer Speed of 180 rpm

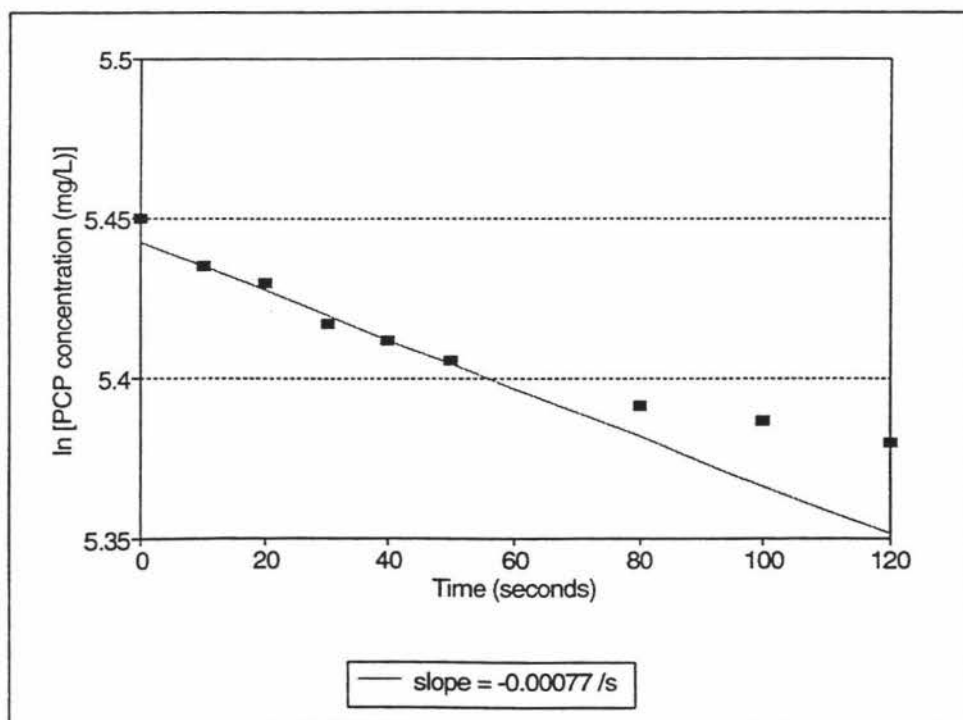


Figure 5.4: Initial Solute Uptake Plot for Stirrer Speed of 390 rpm

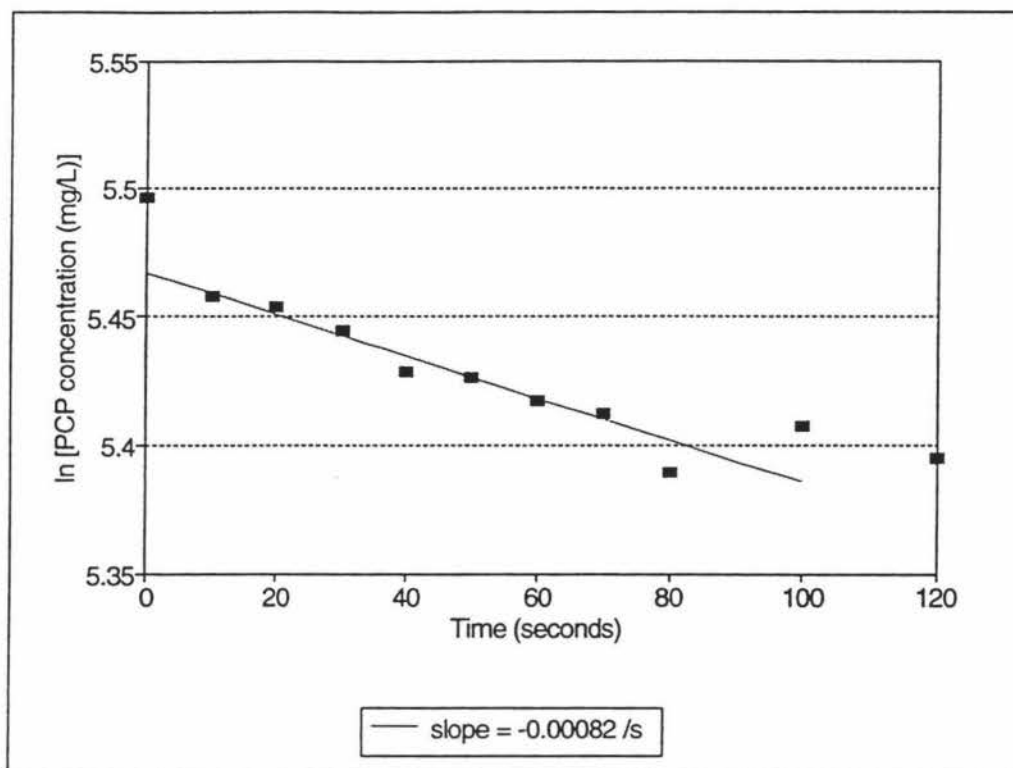


Figure 5.5: Initial Solute Uptake Plot for Stirrer Speed of 560 rpm

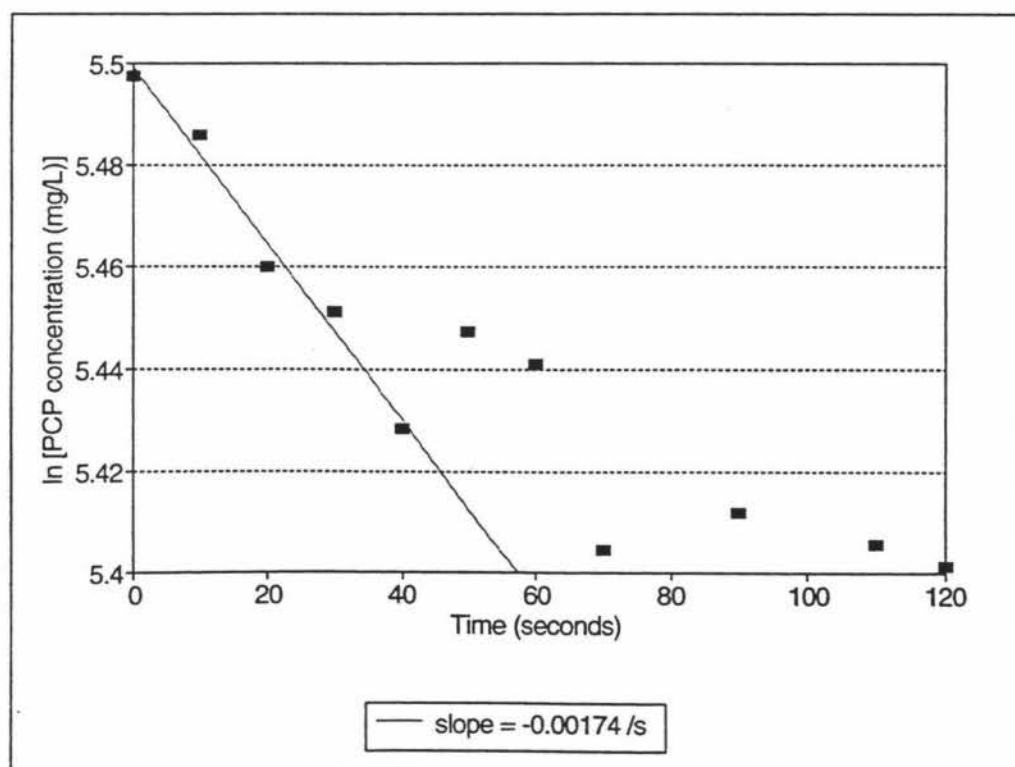


Figure 5.6: Initial Solute Uptake Plot for Stirrer Speed of 760 rpm

5.3.2 Surface Diffusion Coefficients

Once the film diffusion coefficients had been determined from the initial uptake data, the model could be fitted to the whole uptake curve in order to calculate the surface diffusion coefficient, D_s . This was done by varying the parameter $BiF/3$ until the model most closely matched the experimental data. Figures 5.7 to 5.10 show the PCP uptake curves along with the model solutions for the four stirrer speeds. Table 5.2 shows the model input parameters and the calculated surface diffusion coefficients.

Table 5.2: HSDM Input Parameters and Surface Diffusion Coefficients:

Expt. No.	Stirrer Speed	Separation Factor F	$kl \times 10^3$ (cm/s)	Biot Number Bi	$\frac{Bi F}{3}$	$D_s \times 10^9$ (cm ² /s)
1	180	0.708	3.84	317.7	75	2.15
2	390	0.689	5.63	392.0	90	2.26
3	560	0.716	6.02	419.2	100	4.68
4	760	0.716	12.76	272.2	65	4.83

The parameter $BiF/3$ in Table 5.2 above gives an indication of the relative importance of the liquid and solid phase mass transport steps. According to Hand *et al* (1983), values of $BiF/3$ of less than 1 indicate that liquid film mass transfer is the controlling step, while values greater than 100 indicate that surface diffusion is the controlling step. As can be seen from Table 5.2, the values of $BiF/3$ are within the range where both liquid film and surface diffusion are significant. It would be expected that $BiF/3$ would increase with stirrer speed as surface diffusion becomes more limiting. However as shown in Table 5.2 the $BiF/3$ value decreased to 65 in the final experiment. This is most likely due to error in the initial slope calculation as mentioned. $BiF/3$ was found by finding a value which gave a good fit to the

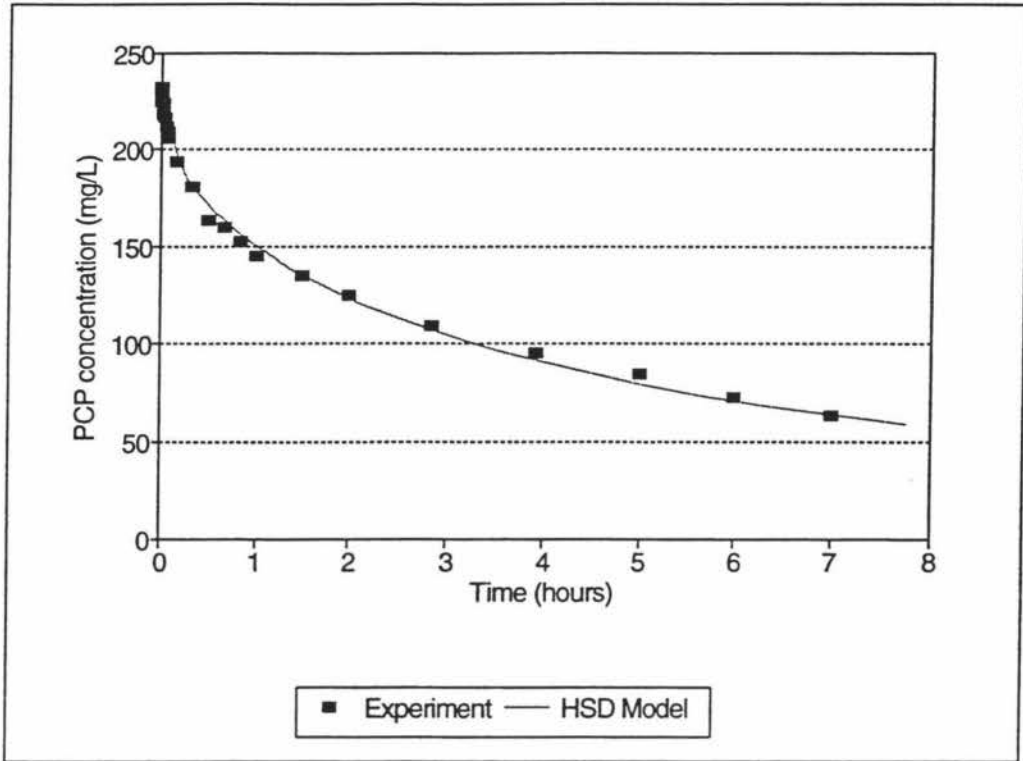


Figure 5.7: Solute Uptake Plot and HSDM solution for Stirrer Speed of 180 rpm

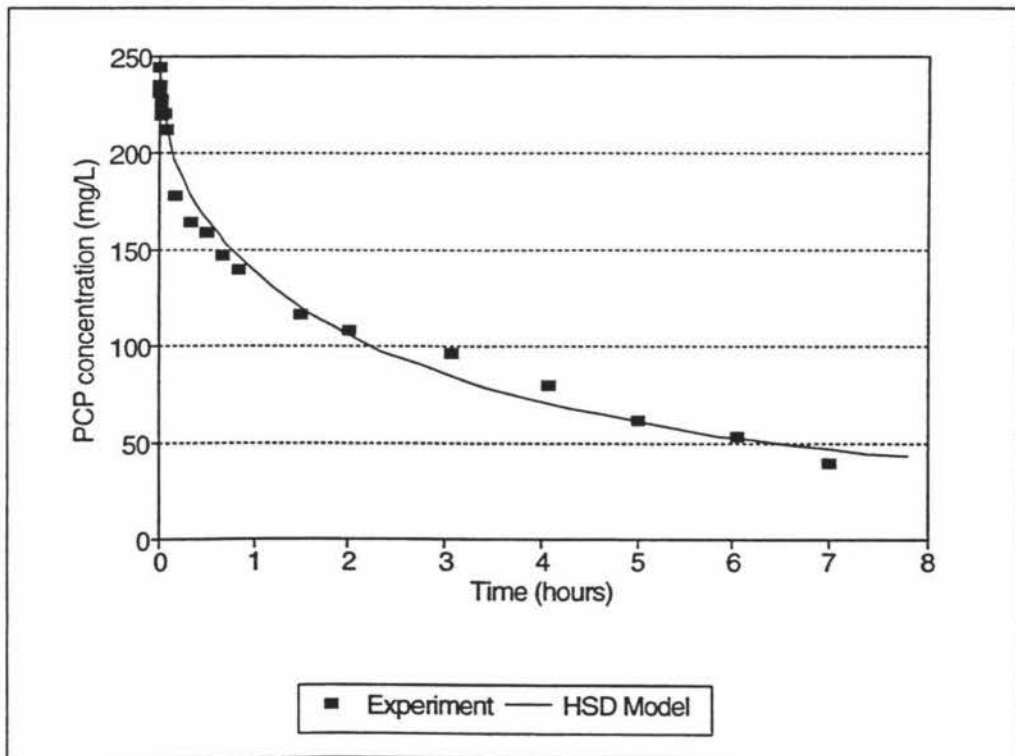


Figure 5.8: Solute Uptake Plot and HSDM solution for Stirrer Speed of 390 rpm

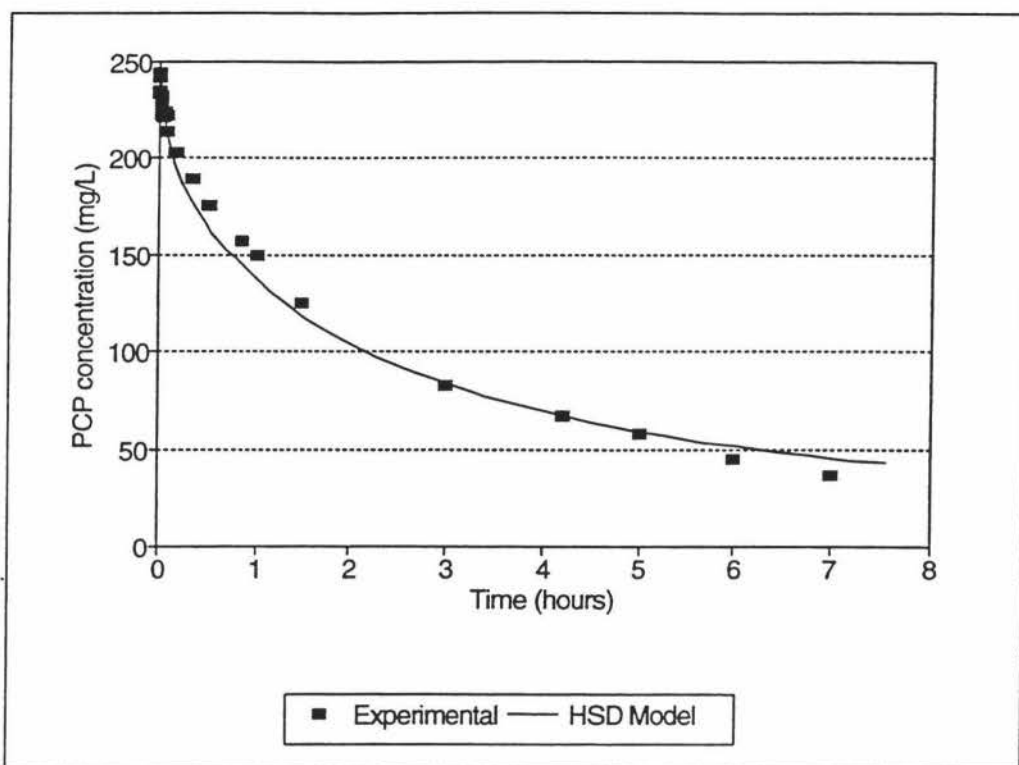


Figure 5.9: Solute Uptake Plot and HSDM solution for Stirrer Speed of 560 rpm

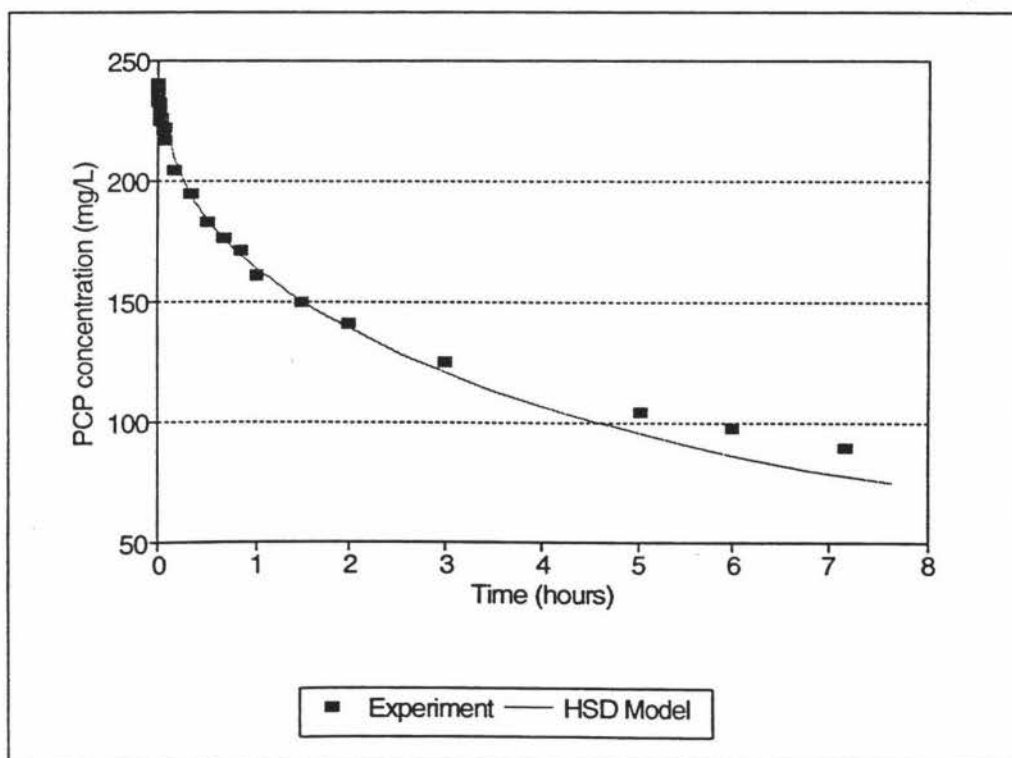


Figure 5.10: Solute Uptake Plot and HSDM solution for Stirrer Speed of 760 rpm

experimental data, given the k_1 value found from the initial slope. As both k_1 and D_s exert an influence on the adsorption rate, there is likely to be more than one combination of initial slope and $BiF/3$ that yields a good fit to the experimental data.

It was decided to use the value of D_s from the second experiment for use in the column model (Chapter 6), as the initial uptake rates for the two experiments with the highest stirrer speeds were too fast to be determined accurately. Hence the D_s values determined at these stirrer speeds were not considered accurate.

The values calculated for k_1 and D_s are of the same order of magnitude as the values for similar compounds found in other kinetic experiments from the literature (Table 5.3).

Table 5.3: Literature Values for k_1 and D_s

<u>Author</u>	<u>Solute</u>	<u>$k_1 \times 10^3$</u> (cm/s)	<u>$D_s \times 10^9$</u> (cm ² /s)	<u>Method</u>
Van Vliet <i>et al</i> (1980)	phenol	7.04	1.24	2 parameter search
Van Vliet & Weber (1981)	toluenesulphonate	4.81	2.33	
	p-chlorophenol	7.45	1.26	
Traegner & Suidan (1989)	p-nitrophenol	6.56	19.15	
Weber and Liang (1983)	p-chlorophenol	7.55	6.29	Microcolumn
	p-nitrophenol	6.22	3.78	
	p-bromophenol	6.50	2.79	

Two methods were used to obtain the kinetic parameters quoted in Table 5.3 above.

The parameters calculated by Van Vliet *et al* (1980), Van Vliet and Weber (1981) and

Traegner and Suidan (1989) were obtained by using a two-parameter search routine to simultaneously find the k_f and D_s values which gave the best fit to experimental batch reactor data, while Weber and Liang (1983) used data from a small column, and assumed that the initial part of the breakthrough curve was dominated by film diffusion in order to calculate k_f . D_s was then found by fitting the model to the experimental breakthrough curve.

Comparing the kinetic parameters of p-chlorophenol and p-nitrophenol found in different studies and shown in Table 5.3 above, the k_f values do not vary significantly between studies, whereas the D_s values do show some variation. The variation is most likely caused by differences in carbon type and particle size. Surface diffusion parameters thus appear to be very system-specific, a result observed by van Vliet and Weber (1981) who found that surface diffusion coefficients varied markedly between different types of activated carbon, while film diffusion coefficients showed very little variation. This effect is most likely due to the extremely heterogeneous internal pore structure of activated carbon. This suggests that for accurate adsorber modelling surface diffusion coefficients must be determined experimentally for the particular adsorbate-adsorbent system of interest.

6. COLUMN STUDIES

6.1 Fixed Bed Adsorbers

Most activated carbon applications involving water and wastewater treatment use a fixed-bed configuration, for reasons of efficiency, economics and ease of operation. The choice of fixed bed contactor is generally made from three types of vessels: closed steel pressure vessels, shallow-bed gravity filter boxes and deep-bed gravity tanks. Pressure vessels used in industry have maximum diameters of around 3.7 metres, with bed volumes ranging from 50 to 1500 m³ (Culp and Clark, 1983). They have the advantage of being able to be operated in an upflow configuration, either in expanded or packed bed mode, and can be fitted into a treatment train with no need for collection, equalisation or re-pumping of the effluent to downstream equipment.

Vessels operating in an upflow expanded bed mode tend to be less susceptible to excessive head loss and fouling with particulate matter than standard packed beds. Also, natural segregation of the activated carbon occurs in expanded beds as more heavily loaded particles concentrate near the bottom of the bed, where they can receive maximum loading in equilibrium with the column influent. This tendency also facilitates the withdrawal of saturated carbon in continuous moving bed systems. Despite these advantages, the downflow mode is often used because careful hydraulic design is required for an upflow system in order to prevent leakage of carbon fines into the effluent.

For larger volume applications in which required contact times are short and reactivation or replacement cycles are long, as is usually the case for taste and odour

control in municipal water treatment, shallow-bed concrete gravity filter-type boxes are often used. In some water treatment plants, a GAC cap is placed on top of the sand in existing filter boxes, or the sand is replaced with GAC altogether. Concrete box-type filter beds may not be suited for applications where long contact times are required, as is the case for many synthetic organic compound removal applications in wastewater treatment. In such cases specially designed deep-bed, large diameter (6 - 9 metres) gravity tanks are more commonly used (Culp and Clark, 1983).

6.2 Fixed Bed Adsorber Operation

The operation of the downflow fixed bed adsorption system is relatively simple. The system can run unattended and can handle a wide variety of flow rates. Normal monitoring comprises pressure drop readings and water sample analysis, the frequency and location of the samples depending on the expected carbon bed life. Samples of influent and effluent are required, while in multi-stage systems interstage samples provide information on the position of the breakthrough curve and indicate when the first stage has been fully loaded. When breakthrough occurs in the final bed, the first bed is taken off line for carbon exchange and a fresh bed is placed at the end of the series.

The major routine operational procedures for fixed bed systems are backwashing and carbon exchange. Periodic backwashing of downflow beds is required in order to alleviate pressure drop across the bed. Uncontaminated water is introduced through the underdrain to effect a 30% bed expansion. In the carbon exchange procedure, the adsorber with spent carbon is isolated and pressurised, and the carbon exits the bottom of the adsorber as a carbon-liquid slurry. The slurry is directed to a

receiving container or transport trailer for reactivation or disposal. The adsorber is refilled with fresh carbon in the same manner and placed back on line or on standby.

Spent carbon can be managed in a number of ways. It can be landfilled or incinerated as a solid waste, or reactivated for reuse. Where recovery of the adsorbed material is not required, thermal reactivation is the most commonly used method of reactivation. Wet oxidation and biological reactivation are two other options, used mainly in powdered activated carbon systems. In most cases an on-site thermal reactivation facility is not cost-effective until more than 4500 kg/day of carbon is required (Stenzel, 1993). Thermal reactivation involves heating the spent carbon up to 980 degrees C in a controlled atmosphere in a multi-hearth furnace or rotary kiln. 10 - 20% losses are generally incurred during the handling and reactivation of granular activated carbon, and the reactivated product sometimes has a lower adsorption capacity than that of virgin material. Reactivation of the carbon with simultaneous recovery of the adsorbate can be achieved by shifting the equilibrium point away from the solid phase with water or a solvent, or steam, in the case of volatile organic compounds.

6.3 Fixed Bed Adsorber Design

If isotherm data establish that carbon adsorption is a viable treatment process, further pilot tests are needed to select the most economical adsorption system design. The most important variables in designing a fixed bed system are the type of adsorbent, hydraulic loading rate and contact time (bed depth). As mentioned, breakthrough curves recorded at various bed depths can be used to determine these parameters. Service time before breakthrough and exhaustion can be plotted against

bed depth (or mass of carbon), and hence the carbon usage rate can be determined as a function of contact time (or bed depth). After the contact time has been established, and the breakthrough curve and carbon usage rate has indicated whether a single bed or staged system is preferred, the designer can select the type of adsorption system that best fits the application.

Conceptual models capable of describing the adsorption process can increase the effectiveness of pilot programs by helping to evaluate the effect of process and operational variables on adsorber performance. The accurate prediction of breakthrough curves by models enables many more configurations to be tested without the need for costly and time-consuming pilot trials. The shape of the breakthrough curve and the rate at which it travels down the bed depends upon the influent conditions, adsorption rate and equilibrium capacity of the particular system. Modelling of breakthrough curves is therefore dependant on knowledge of adsorption equilibrium and kinetic properties.

6.4 Homogeneous Surface Diffusion Model Applied to Fixed-Bed Adsorbers

Having determined the equilibrium and kinetic properties of the PCP system in the previous two chapters, it is possible to apply the homogeneous surface diffusion equation (HSDM) to a fixed bed adsorber. As mentioned, the HSDM has been used to model many fixed bed adsorption systems in previous studies. The equations that describe adsorption dynamics in a fixed bed adsorber are developed from liquid and solid phase mass balances taken across an element of infinitesimal thickness normal to the direction of flow. In the homogeneous surface diffusion model the following assumptions are made when conducting the mass balances:

- i. Molecular diffusion and hydrodynamic dispersion represented by an axial dispersion coefficient.
- ii. No radial concentration gradients.
- iii. Intraparticle transport described by surface diffusion.
- iv. Liquid diffusion resistance described by film transfer.
- v. Instantaneous equilibrium at the interface between the adsorbate and the adsorbent.

Considering the above assumptions, the governing mass balance equations for the particle and the adsorber are:

Particle:

$$\frac{\partial q}{\partial t} = D_s \frac{\partial}{\partial r} \left(r^2 \frac{\partial q}{\partial r} \right) \quad (6.1)$$

Adsorber:

$$\frac{\partial C}{\partial t} = D_L \frac{\partial^2 C}{\partial z^2} - v \frac{\partial C}{\partial z} - \frac{3(1 - \epsilon)}{\epsilon R} k_f (C - C_s) \quad (6.2)$$

Where D_L is the axial dispersion coefficient, v is the interstitial fluid velocity, and ϵ is the void fraction of the bed.

Boundary conditions for the above equations are:

at $t = 0$:

$$q = C = 0 \quad (6.3)$$

at $r = 0$:

$$\frac{\partial q}{\partial r} = 0 \quad (6.4)$$

at $r = R$:

$$\rho_p A D_s \frac{\partial q}{\partial r} = k_l A (C - C_s) \quad (6.5)$$

$$q_s = K C_s^{1/n} \quad (6.6)$$

at $z = 0$:

$$D_L \frac{\partial C}{\partial z} = -v(C_o - C) \quad (6.7)$$

at $z = L$:

$$\frac{\partial C}{\partial z} = 0 \quad (6.8)$$

In order to simplify the solution of the above equations the following dimensionless variables are introduced:

$$C^* = \frac{C}{C_o} ; C_s^* = \frac{C_s}{C_o} ; q^* = \frac{q}{q_o} ; q_s^* = \frac{q_s}{q_o} \quad (6.9)$$

$$r^* = \frac{r}{R} ; z^* = \frac{z}{L} ; \tau = \frac{D_s t}{R^2} \quad (6.10)$$

The various equilibrium, kinetic and physical parameters are arranged into four dimensionless groups, listed in Table 6.1 below.

Table 6.1: HSDM Dimensionless Groups

Dimensionless Group	Equation	Mass Transfer Mechanisms Represented
Pe	vL/D_L	Convection/Dispersion
ψ	$k_f R/D_s$	Film diffusion/Surface diffusion
ω	vR^2/LD_s	Convection/Surface diffusion
σ	$\rho_p q_0/C_0$	Equilibrium Capacity

The Peclet number Pe represents the ratio of convection to hydrodynamic dispersion in the column. ψ represents the ratio of the rates of film transfer and surface diffusion. ω represents the ratio of convection to surface diffusion. It contains the parameter L/v , the adsorber contact time. σ represents the capacity of the adsorbent. It is determined from equilibrium experiments. For a particular contact time and hydraulic loading rate, σ determines the amount of carbon required to treat a given volume of water.

By introducing the above parameters, Equations (6.1) and (6.2) become:

$$\frac{\partial q^*}{\partial \tau} = \frac{1}{r^{*2}} \frac{\partial}{\partial r} \left(r^{*2} \frac{\partial q}{\partial r^*} \right) \quad (6.11)$$

$$\frac{\partial C^*}{\partial \tau} = \frac{\omega}{Pe} \frac{\partial^2 C^*}{\partial z^{*2}} - \omega \frac{\partial C}{\partial z^*} - \frac{3(1 - \epsilon)}{\epsilon} \psi [C^* - C_s^*] \quad (6.12)$$

The dimensionless initial and boundary conditions are:

at $\tau = 0$:

$$C^* = q^* = 0 \quad (6.13)$$

at $r^* = 0$:

$$\frac{\partial q^*}{\partial r^*} = 0 \quad (6.14)$$

at $z^* = 0$:

$$\frac{\partial C^*}{\partial z^*} = -Pe(1 - C^*) \quad (6.15)$$

at $r^* = 1$:

$$\frac{\partial q^*}{\partial r^*} = \frac{\Psi}{\sigma}(C^* - C_s^*) ; q_s^* = C_s^{*(1/n)} \quad (6.16)$$

at $z^* = 1$:

$$\frac{\partial C^*}{\partial z^*} = 0 \quad (6.17)$$

The above model equations were solved using a combination of orthogonal collocation, Newton-Raphson and numerical integration techniques.

6.5 Model Parameter Determination

In order to solve the above equations various parameters are required: The equilibrium parameters K and $1/n$, the kinetic parameters k_f and D_s , and the column parameters D_f , ε and R .

The equilibrium parameters were determined from isotherm experiments (Chapter 4). The surface diffusion coefficient, D_s , was determined from batch kinetic experiments (Chapter 5). The film transfer coefficient, k_f , was determined from empirical correlations found in the literature (Roberts *et al*, 1985).

6.5.1 Film Transfer Coefficient

In most correlations k_f is incorporated in the dimensionless Sherwood number, Sh , which is predicted as a function of the Reynolds number, Re , and the Schmidt number, Sc . Re and Sc characterise the hydrodynamic conditions in the column and molecular diffusion in the solution respectively. Roberts *et al* (1985) compared four such correlations with experimental data and found that the correlation proposed by Gnielinski gave the best prediction of k_f in water treatment situations. This correlation is (in simplified form):

$$Sh = (2 + 0.644 Re^{1/2} Sc^{1/3})[1 + 1.5(1 - \epsilon)] \quad (6.18)$$

where:

$$Re = \frac{2R\rho_f v}{\mu_f} ; \quad Sc = \frac{\mu_f}{\rho_f D_m} ; \quad Sh = \frac{2Rk_f}{D_m} \quad (6.20)$$

This correlation is valid for Reynolds numbers of 1 to 10,000 and Schmidt numbers from 0.6 to 10,000 (Roberts *et al*, 1985). Re , Sc and k_f values for the column experiments are listed in Appendix 3.

The Schmidt and Sherwood numbers in equations (6.20) contain the parameter D_m , which is the molecular diffusivity of the solute in water. This parameter was determined using the correlation of Wilke and Chang (1955) for dilute aqueous solutions, used in previous investigations (Crittendon and Weber, 1978; Roberts *et al*, 1985):

$$D_m = 7.4 \times 10^{-8} \frac{(\phi M_B)^{1/2}}{V_A \mu^{0.6}} \quad (6.20)$$

V_A is the molar volume of the solute at normal boiling point (cm^3/gmol), μ is the viscosity of the solution (cP), and M_B is the molecular weight of the solvent. The method proposed by Fedor (1979) was used to estimate V_A .

6.5.2 Dispersion Coefficient

Dispersion effects are represented in the model by the column Peclet number, vL/D_L . In packed beds the reciprocal of the particle Peclet number, D_L/vR , is approximately equal to 2 over a wide range of Reynolds numbers, 0.1 to 50 (Levenspiel, 1972). Therefore the column Peclet number is approximately constant and equal to $L/2R$.

Alternatively the Peclet number can be estimated by using correlations to estimate the column dispersion coefficient D_L . One such correlation was proposed by Fried (1975) and used by Sursala (1994) to model dispersion effects in soil columns:

$$D_L = D_m [0.67 + 0.5(\text{Re Sc})^{1.2}] \quad (6.21)$$

The correlation of Levenspiel (1972) was used to simulate dispersion effects in the model. Dispersion coefficient values for both the Levenspiel and Fried correlations are listed in Appendix 3.

6.6 Experimental and Predicted Breakthrough Curves

Three column experiments were undertaken at varying flow rates. PCP solution was pumped from a reservoir through a 6 cm long column of activated carbon, and the effluent concentration was monitored at regular intervals (see section 3.4). Table 6.2 shows the model input parameters for the three column runs.

Table 6.2: Fixed-Bed Model Input Parameters

C_o (mg/l)	Q (ml/min)	v (cm/s)	D_L (cm ² /s)	ω	ψ	σ	Pe
200	2.80	0.15	0.022	14283	18086	1004	43
200	5.07	0.25	0.036	23463	27257	1001	43
200	6.15	0.33	0.048	30756	24921	1000	43

The curves have been normalised by plotting relative concentration (C/C_o) versus a throughput parameter defined as:

$$T = \frac{t}{\theta R_f} \quad (6.23)$$

Where

$$\theta = \text{ResidenceTime} = \frac{L}{v} ; R_f = \text{Retardation Factor} = \frac{\sigma(1 - \epsilon)}{\epsilon}$$

R_f represents the maximum amount of solute that the column can adsorb, expressed as a number of bed void volumes of influent. The parameter t/θ represents the

number of bed void volumes passed through the column. Thus if there was perfect plug flow with no dispersion and instantaneous adsorption, it would be expected that the breakthrough curve would resemble a vertical line at throughput parameter $T = 1$. Dispersion of solute along the column and slow rates of mass transfer from the solution to the adsorbent surface cause solute to break through a lot earlier than this, thus causing the breakthrough curve to spread out.

Figures 6.1 to 6.3 show the experimental breakthrough curves, along with the model predictions using the input parameters detailed above.

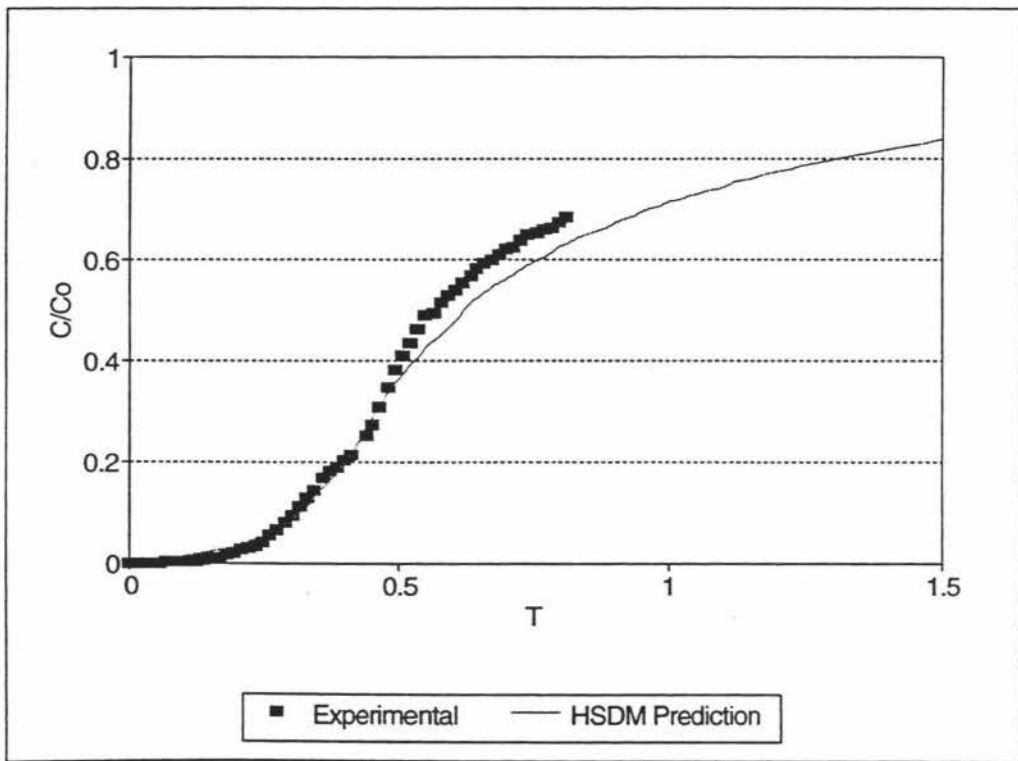


Figure 6.1: PCP Breakthrough Curve, Flow Rate = 2.80 ml/min

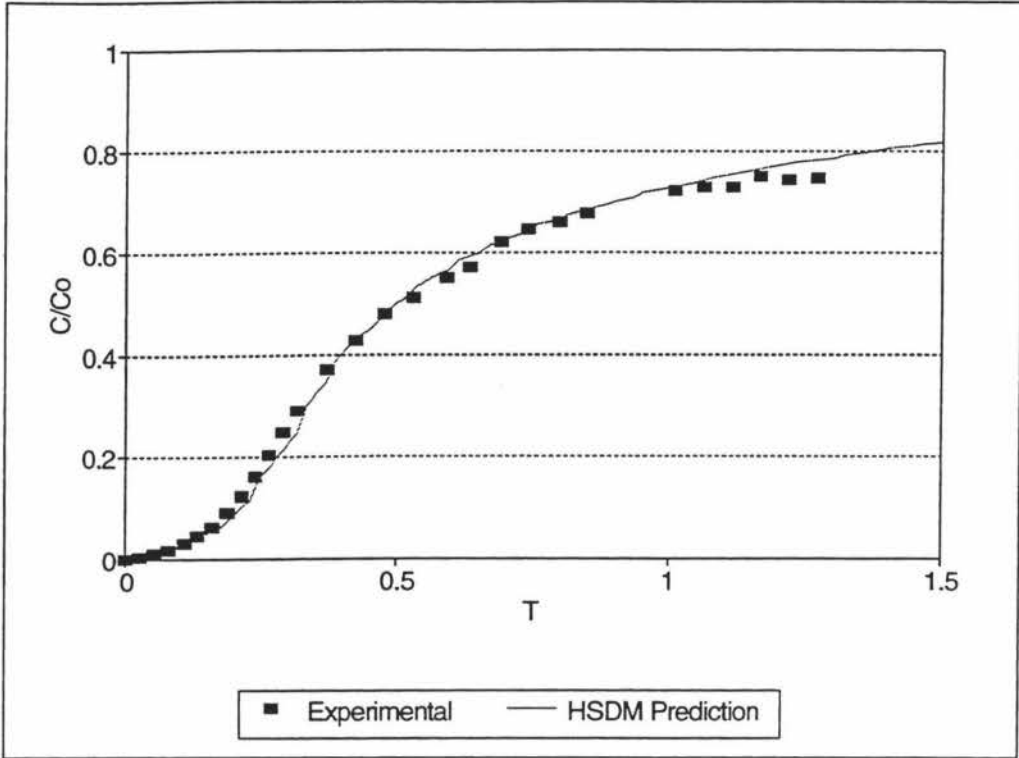


Figure 6.2: PCP Breakthrough Curve, Flow Rate = 5.07 ml/min

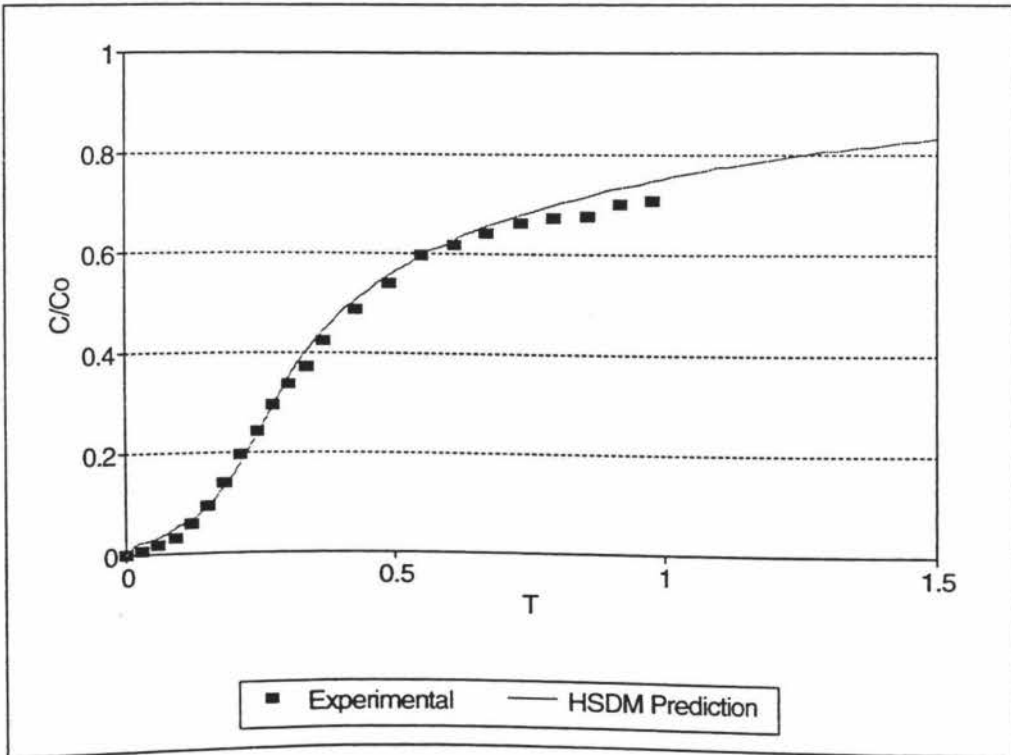


Figure 6.3: PCP Breakthrough Curve, Flow Rate = 6.15 ml/min

As is shown in the above figures, the HSDM generally gave a good prediction of the breakthrough curves. The discrepancy between the experimental data and the model prediction in Figure 6.1 is thought to have been caused by a pump malfunction which caused a momentary backflow in the column. This backflow may have flushed some of the adsorbed solute from the column, which would explain the sudden rise in effluent concentration at approximately $T = 0.5$.

6.6.1 Effect of Hydraulic Loading

The effect of increasing the hydraulic loading of the column is to spread the breakthrough curve, with the solute breaking through at lower throughputs (Figure 6.4). The spreading of the curve at high hydraulic loading rates is due to the adsorption rate becoming more limited by film transfer and surface diffusion.

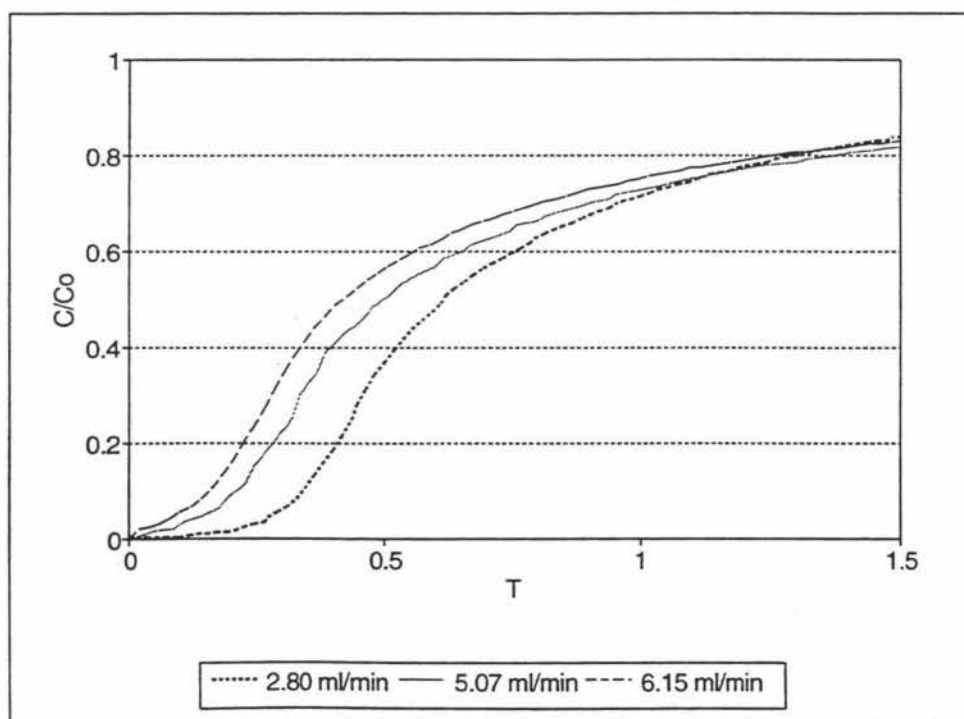


Figure 6.4: Effect of Flow Rate on the Breakthrough Curve

Figure 6.5 shows the relationship between the hydraulic loading rate and throughput until breakthrough and exhaustion of the column. Breakthrough was assumed to occur when the effluent concentration had reached 10% of the influent concentration, while column exhaustion was assumed to occur when the effluent had reached 90% of the influent concentration. The two curves indicate that the breakthrough point is a lot more sensitive to the hydraulic loading rate than the exhaustion point.

The x intercept of the lower line in Figure 6.5 represents the maximum hydraulic loading rate that can be applied to this particular length of column without the solute breaking through immediately. For any particular bed length, the hydraulic loading rate should be below this maximum value, with any decrease in hydraulic loading rate yielding greater efficiency in terms of carbon utilization, however at a cost of larger equipment size and carbon inventory.

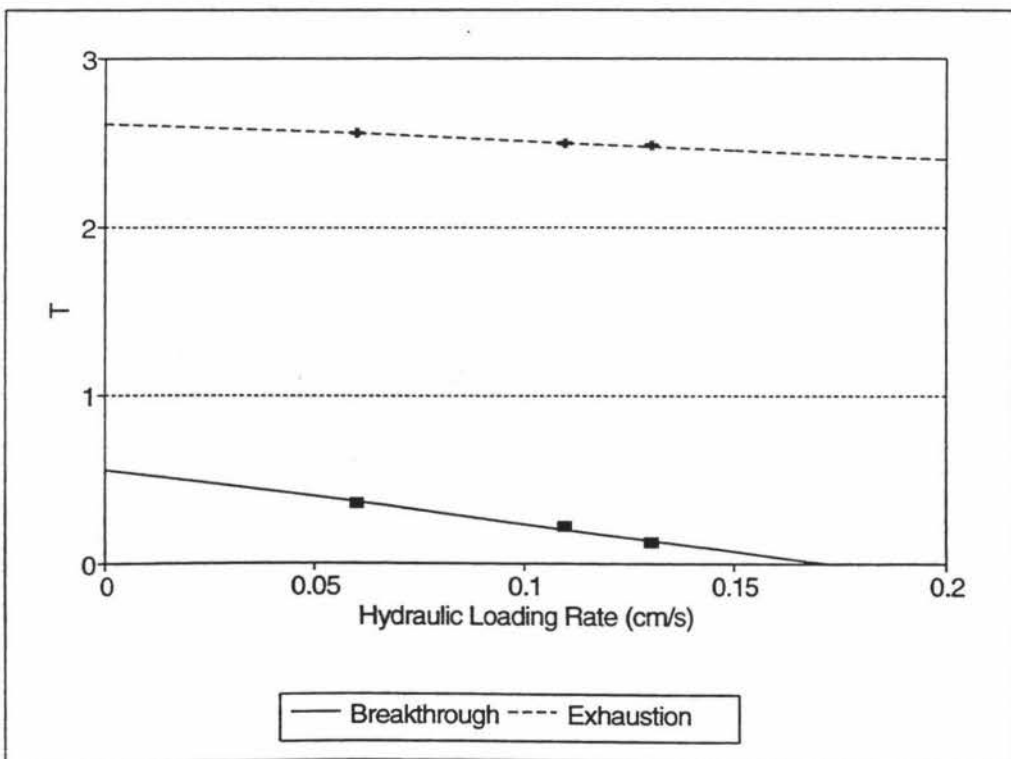


Figure 6.5: Effect of Hydraulic Loading rate on Breakthrough and Exhaustion Throughputs

6.6.2 Effect of Dispersion

The breakthrough curves were found not to be sensitive to changes in Pe , indicating that axial dispersion is not a limiting transport mechanism for the range of flow rates studied. This corresponds with the findings of Crittendon and Weber (1978) and Liu and Weber (1981) that dispersion effects are not significant in most adsorption column applications. The choice of correlation used to determine D_L and hence Pe had no significant effect on the shape of the breakthrough curve.

6.6.3 Effect of Film Transfer Coefficient

Liquid film transfer appears to have little effect on the breakthrough curve. According to Crittendon and Weber (1978) and Hand *et al* (1984), the Biot number (ψ/σ) must be less than 0.5 for film transfer to control the adsorption rate, and above 30 for intraparticle diffusion to control the rate. In this system the Biot number ranged from 18.0 to 27.2, indicating that the adsorption rate was controlled more by intraparticle diffusion than film transfer. Figure 6.6 shows the effect of different film transfer coefficient correlations on the predicted breakthrough curve for the experiment with the lowest Biot number (18.0). As can be seen, the choice of correlation to determine k_f has only a small effect on the initial portion of the breakthrough curve.

The two correlations used were those of Gnielinski and Wilson, as these gave the widest range of k_f values. Gnielinski yielded a k_f value of 1.13×10^{-3} cm/s and Wilson 1.52×10^{-3} cm/s. Gnielinski's correlation gave a slightly better fit to the experimental data than that of Wilson, a result found in previous studies (Roberts *et al*, 1985). k_f values using both correlations are listed in Appendix 3.

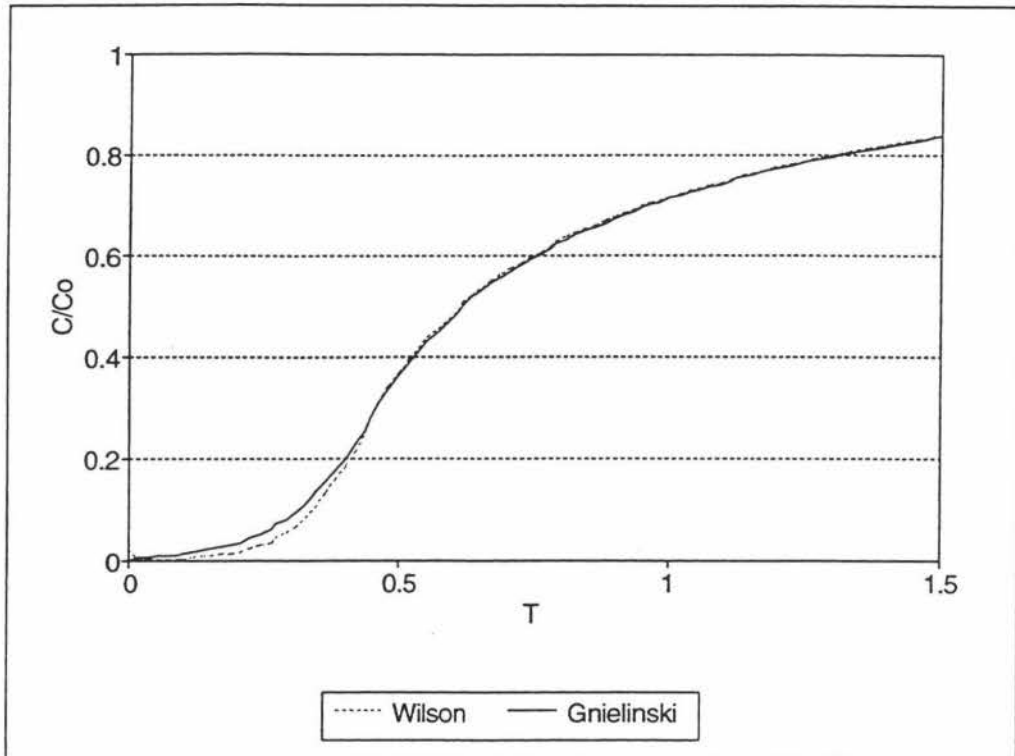


Figure 6.6: Effect of different k_f Correlations on the Breakthrough Curve

6.6.4 Effect of Surface Diffusion Coefficient

The breakthrough curves were very sensitive to the surface diffusion coefficient value, indicating that surface diffusion is the rate limiting step for the system under investigation. This is demonstrated in Figure 6.7 below, where the D_s value is increased by 35%, the same increase as was used for the film transfer coefficients in the previous section. As can be seen, the effect of increasing D_s is to delay solute breakthrough, indicating that surface diffusion is the rate limiting step.

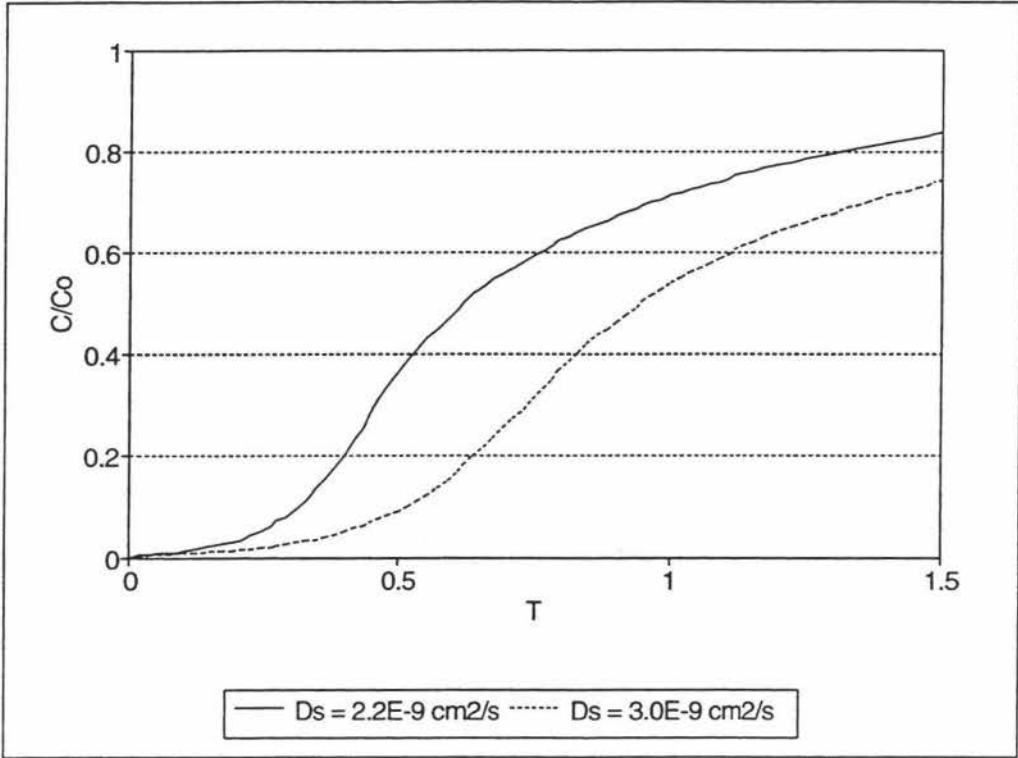


Figure 6.7: Effect of D_s on the Breakthrough Curve

6.7 Applications of the Model

Once the model has been verified on a pilot scale, full-scale adsorber performance can be predicted using the model instead of expensive pilot plant trials. This information can be used to design full-scale adsorption systems. For example bed depth service time curves could be determined for different hydraulic loading rates. From these curves the carbon exhaustion rate per unit volume of throughput could be established as a function of bed length as follows:

$$\frac{\text{Mass Carbon}}{\text{Throughput}} (\text{kg/m}^3) = \frac{L - \text{MTZ}}{L} \frac{1}{TKC_o^{(1/n-1)}} \quad (6.24)$$

Where T is the throughput parameter for breakthrough at a particular bed length,

and MTZ is the length of the mass transfer zone. The length of the mass transfer zone would determine if multiple stages are necessary in order to achieve an acceptable carbon utilisation. The effect that different adsorbents and influent concentrations have on adsorber performance can also be assessed by varying σ .

It must be remembered, however, that adsorption behaviour is very system-specific and adsorption capacity and rate will vary depending on the application and type of water being treated. In particular, the presence of other dissolved contaminants will reduce the effective capacity of the carbon for the target contaminant. The extent of this reduction is hard to predict, and so modelling multi-contaminant systems such as those found in practical water treatment applications is difficult. However the modelling of complicated systems must be based on an accurate description of simple single-component systems. The homogeneous surface diffusion model has described the simple PCP-water system well and could be used as a starting point for planning pilot programs and providing preliminary cost estimates for full-scale applications.

7. CONCLUSIONS

The effective and efficient design of fixed-bed adsorbers is based on an accurate description of the adsorption process. Mathematical models based on external and internal mass transfer steps and using experimentally determined equilibrium and kinetic parameters have proven useful in describing fixed bed behaviour. Once verified experimentally, models can be used to plan pilot programs and to assess the effectiveness of different adsorber configurations. One model that has been successful in describing a wide range of adsorption systems is the homogenous surface diffusion model (HSDM). The HSDM has been used in this study to successfully predict the breakthrough curves of pentachlorophenol (PCP) in bench scale activated carbon adsorption column studies.

The use of the HSDM to predict fixed-bed behaviour depends on accurate determination of equilibrium and mass transfer parameters, and these were determined using batch equilibrium and kinetic experiments. The equilibrium capacity of granular activated carbon was found to best fit the Freundlich isotherm model, with coefficients of $K = 95.0$ and $1/n = 0.180$. These values were consistent with the Freundlich coefficients for similar compounds found in the literature. Surface diffusion and film transfer coefficients were obtained by fitting the HSDM to batch adsorption data.

In modelling column performance, it was found that the rate of adsorption was primarily limited by surface diffusion. Gnielinski's correlation for the external film transfer coefficient was found to give the best fit to the experimental data, although the impact on the predicted breakthrough curve of varying the film transfer

coefficient was not great. The role of axial dispersion was found to be insignificant in the system studied, a finding consistent with other investigations.

The study has confirmed the conclusions of other investigations that the HSDM is a useful tool for predicting adsorber performance. Practical applications involve multi-contaminant systems many times more complicated than the one studied. However the study of simple single-component systems provides a basis for further study into more complicated effects. If any applications for PCP removal from water were to arise then the parameters determined in this study could be used in conjunction with the HSDM to provide a guide to the scope and size of the adsorber system required and to plan further pilot plant studies.

LIST OF SYMBOLS

A	Adsorbent surface area	cm ²
Bi	Biot number, k_1AR^2/VD_s	
C	Bulk solution concentration	mg/l
C ₀	Initial solution concentration	mg/l
C _s	Solution concentration adjacent to adsorbent surface	mg/l
C [*]	Dimensionless concentration, C/C_0	
C _s [*]	Dimensionless concentration adjacent to surface, C_s/C_0	
D _L	Dispersion coefficient	cm ² /s
D _M	Molecular diffusivity	cm ² /s
D _s	Surface diffusion coefficient	cm ² /s
F	Dimensionless separation factor	
k ₁	Film diffusion coefficient	cm/s
K	Freundlich isotherm coefficient	
L	Column length	cm
M _B	Molecular weight of solvent	g/gmol
n	Freundlich isotherm coefficient	
Pe	Peclet number, vL/D_L	
q	Adsorbed solute concentration	mg/g
q ₀	Adsorbed solute concentration in equilibrium with initial solution concentration C ₀	mg/g
q _s	Adsorbed solute concentration at adsorbent surface	mg/g
q [*]	Dimensionless adsorbed solute concentration, q/q_0	
q _s [*]	Dimensionless adsorbed solute concentration at surface, q_s/q_0	
Q	Column feed flow rate	ml/min

r	Radial position within particle	cm
r^*	Dimensionless radial coordinate, r/R	
R	Adsorbent particle radius	cm
Re	Reynolds number	
Sc	Schmidt number	
Sh	Sherwood number	
t	time	s
T	Temperature	K
v	Interstitial fluid velocity	cm/s
V	Volume of batch reactor	L
V_A	Molar volume of solute at normal boiling point	ml/mol
W	Weight of adsorbent	g
z	Axial position along column	cm
z^*	Dimensionless axial coordinate, z/L	
ϵ	Bed voidage	
ρ	Solution density	g/L
ρ_p	Particle density	g/cm ³
τ	Dimensionless time, $D_s t/R^2$	
ψ	film transfer rate/surface diffusion rate, $k_f R/D_s$	
σ	Separation factor, $\rho_p q_o/C_o$	
ω	Convection rate/surface diffusion rate, vR^2/LD_s	
ϕ	Association factor (=2.6 for water)	
μ	Solution viscosity	kg/ms

REFERENCES

- ANZECC and NATIONAL HEALTH & MEDICAL RESEARCH COUNCIL, 1992.
Australian and New Zealand Guidelines for the Assessment and Management of Contaminated Sites.
- ARMISHAW, R.F. *et al*, 1994. Soil and Groundwater Studies at some CCA Timber Treatment Sites, *Water and Wastes in NZ*, March, 44-48.
- BHASKAR, G.V. and BHAMIDIMARRI, R.S, 1992. Adsorption of 2,4-D onto Activated Carbon: Application of Nth Order Approximation, *J. Chem. Tech. Biotechnol.*, 53, 297-300.
- BHASKAR, G.V. and BHAMIDIMARRI, R.S, 1991. A Simple Driving Force Model for Activated Carbon Adsorption, *Chemica 91 Proceedings*, 558-565.
- COTRUVO, J.A. and VOGT, C., Development of Revised Primary Drinking Water Regulations, *Jour. AWWA*, November 1984,34-38.
- CRITTENDON, J.C. *et al*, 1986. Design of Rapid Small-Scale Adsorption Tests for a Constant Diffusivity, *J. Water Poll. Control Fed.*, 58, 312-319.
- CRITTENDON, J.C. *et al*, 1993. Removal of Dissolved Organic Carbon using Granular Activated Carbon, *Wat. Res.*, 27, 715-721.

- CRITTENDON, J.C. and WEBER, W.J., 1978. Predictive Model for Design of Fixed-Bed Adsorbers: Parameter Estimation and Model Development, *J. Env. Eng. Div., ASCE*, 104,185-197.
- CRITTENDON, J.C. *et al*, 1991. Predicting GAC Performance with Small-Scale Column Tests, *Jour. AWWA.*, Jan, 77-87.
- CRITTENDON, J.C. and WEBER, W.J., 1978. Predictive Model for Design of Fixed-Bed Adsorbers: Single Component Model Verification, *J. Env. Eng. Div., ASCE*, 104,433-443.
- CULP, R.J. and CLARK, R.M., 1983. Granular Activated Carbon Installations, *Jour. AWWA*, August, 398-405.
- DAHAB, M.F. *et al*, 1991. Treatment of a Wood Products Superfund Wastewater: A Case Study, *Can. J. Civ. Eng.*, 18, 654-662.
- DRENT, R., 1994. Toxic Site Cleanup Alarm, *Sunday Star-Times*, 6 November.
- ECKENFELDER, W., 1980. *Principles of Water Quality Management*, CBI, Boston.
- FAMULARO, J. *et al*, 1980. Prediction of Carbon Column Performance from Pure Solute Data, *J. Water Poll. Control Fed.*, 52, 2019-2032.
- FEDORS, R.F., 1979. A Method to Estimate Critical Volumes, *AIChE. J.*, 25, 202

- FETTIG, J. and SONTHEIMER, H., 1987. Kinetics of Adsorption on Activated Carbon: I. Single-Solute Systems, *J. Env. Eng. Div., ASCE*, 113, 764-779.
- FRIED, J.J., *Groundwater Pollution*, Elsevier Scientific, Amsterdam.
- GRAHAM, J.R. and RAMARATNAM, M., 1993. Recover VOCs Using Activated Carbon, *Chem. Eng.*, February, 6-12.
- HAND, D.W. *et al*, 1984. Simplified Models for Design of Fixed-Bed Adsorption Systems, *J. Env. Eng Div., ASCE*, 110, 440-456.
- HAND, D.W. *et al*, 1983. User-Oriented Batch Reactor Solutions to the Homogeneous Surface Diffusion Model, *J. Env. Eng. Div., ASCE*, 109, 82-101.
- HOPPER, D.R., 1989. Cleaning Up Contaminated Waste Sites, *Chem. Eng.*, August, 94-110.
- HOSSAIN, M.A. and YONGE, D.R., 1992. Finite Element Modeling of Single Solute Activated Carbon Adsorption, *J. Env. Eng. Div., ASCE*, 118, 238-253.
- HUSER, B., 1992. Contamination from the Use of Timber Treatment Chemicals, *Water and Wastes in NZ*, September, 22-28.
- ISRAELACHVILI, J.N., 1985. *Intermolecular and Surface Forces*, Academic Press, London.

- ISRAELACHVILI, J.N. and NINHAM, B.W., 1977. Intermolecular Forces-the Long and Short of It, *J. Colloid and Interface. Sci.*, 58, 14-25
- JORENS, P.G. and SCHEPENS, P.J.C., 1993. Human Pentachlorophenol Poisoning, *Human & Environ. Toxicol.*, 12, 479-495.
- LEVENSPIEL, O., 1972. *Chemical Reaction Engineering* (2nd Edition), Wiley, New York.
- LIU, K. and WEBER, W.J., 1981. Characterisation of Mass Transfer Parameters for Adsorber Modeling and Design, *J. Water Poll. Control Fed.*, 53, 1541-1550.
- MACKIE, J.A. and NIESON, K., 1984. Hazardous Waste Management: The Alternatives, *Chem. Eng.*, August 6, 1984, 50-64.
- MADRAS, G. *et al*, 1994. Supercritical Extraction of Organic Contaminants from Soil Combined with Adsorption onto Activated Carbon, *Environ. Prog.*, 13,45-50.
- McKINNON, R.J. and DYKSEN, J.E., 1984. Removing Organics from Groundwater through Aeration Plus GAC, *Jour. AWWA*, May, 42-47.
- MILLER,S., 1980. Adsorption on Carbon: Theoretical Considerations. *Environ. Sci. Technol*, 21, 910-914
- MILTON, R.J *et al*, 1989. Treatment of Seasonal Pesticides in surface Waters, *Jr. AWWA*, January, 43-52.

MINISTRY FOR THE ENVIRONMENT, 1992. Report of the National Task Group Investigating Site Contamination from the Use of Timber Treatment Chemicals.

NOLL, K, GOUNARIS,V, HOU,W, 1992. *Adsorptio Technology*, Lewis Publishers, Michigan.

O'BRIEN, R.P. and FISHER, J.L., 1983. There is an Answer to Groundwater Contamination, *Water Eng. Man.*, May, 30-70.

O'BRIEN, G.J., 1992. Estimation of the Removal of Organic Priority Pollutants by the Powdered Activated Carbon Treatment Process, *Water Env. Res.*, 64, 877-882.

PEEL R.G. *et al*, 1981. A Branched Pore Kinetic Model for Activated Carbon Adsorption, *AIChE. J.*, 27, 26-32.

PEEL, R.G. and BENEDEK, A., 1981. A Simplified Driving Force Model for Activated Carbon Adsorption, *Can. Jour. Chem. Eng.*, 59, 688-692.

PIRBAZARI, M. *et al*, 1991. GAC Adsorber Design for Removal of Chlorinated Pesticides, *J. Env. Eng. Div. (ASCE)*, 117, 80-100.

RANDTKE, S.J. and SNOEYINK, V.L., 1983. Evaluating GAC Adsorptive Capacity, *Jour. AWWA*, 406-413.

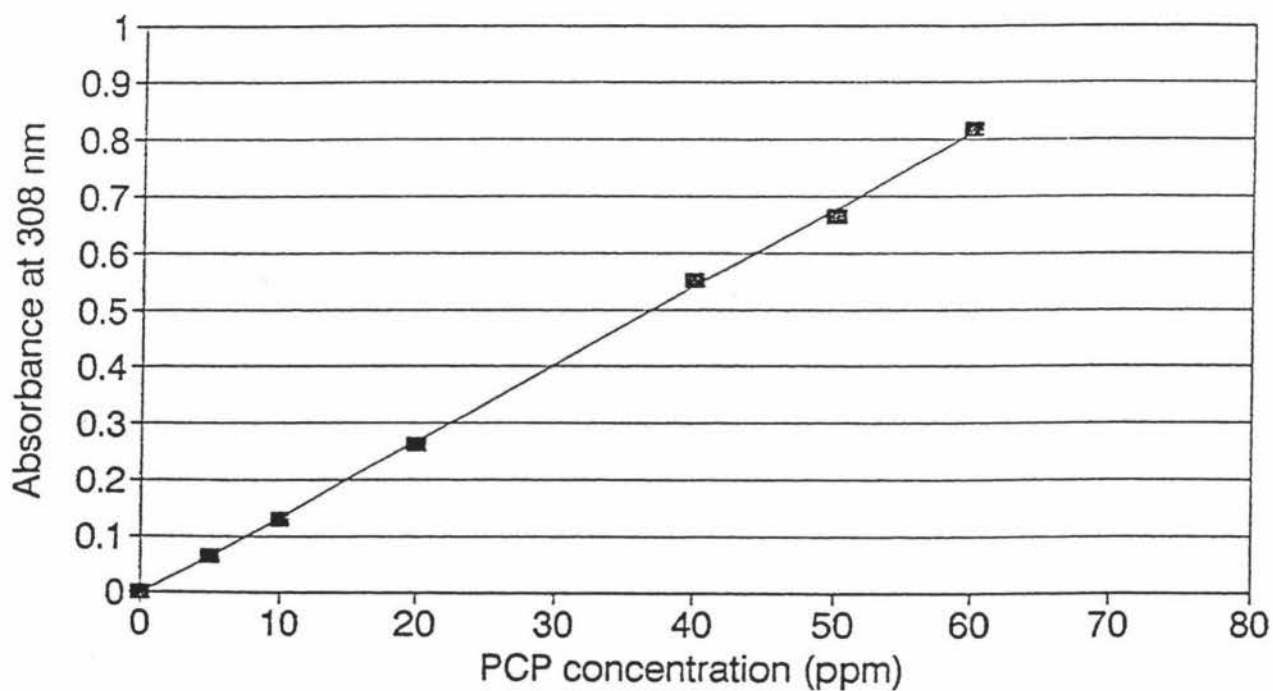
- ROBERTS, P.V. *et al*, 1985. External Mass-Transfer Rate in Fixed-Bed Adsorption, *J. Env. Eng. Div., ASCE*, 111, 891-905.
- ROY, D *et al*, 1993. A Simplified Solution Technique for Carbon Adsorption Model, *Wat. Res.*, 27, 1033-1040.
- SMITH, E.H. *et al*, 1987. Modeling the Adsorption of Target Compounds by GAC in the Presence of Background Dissolved Organic Matter, *Environ. Prog.*, 6, 18-25.
- SORIAL, G.A. *et al*, 1993. Effect of GAC Characteristics on Adsorption of Organic Pollutants, *Water Env. Res.*, 65, 53-57.
- SPETH, T.F. and MILTNER, R.J., 1990. Technical Note: Adsorption Capacity of GAC for synthetic Adsorbents, *Jour. AWWA.*, Feb, 72-75.
- STENZEL, M.H. and MERZ, W.J., 1989. Use of Carbon Adsorption Processes in Groundwater Treatment, *Environ. Prog.*, 8, 257-264.
- STENZEL, M.H., 1993. Remove Organics by Activated Carbon Adsorption, *Chem. Eng. Prog.*, April, 36-43.
- STEVENSON, P., 1993. "No Risk to Employees' Health", *Terra Nova*, July, 24-35.
- STEVENSON, P., 1993. The Scandal of the PCP Dumps, *Terra Nova*, May, 10-15.

- STEVENSON, P., 1993. PCP's: Crunch Time for the Timber Industry, *Terra Nova*, July, 13-23.
- SURSULA, S., 1994. Adsorption-Desorption Characteristics of Phenoxyacetic Acids and Chlorophenols in a Volcanic Soil, PhD Thesis, Massey University, New Zealand.
- SYMONS, J.M., 1984. A History of the Attempted Federal Regulation Requiring GAC Adsorption for Water Treatment, *Jour. AWWA*, August, 34-43.
- SZABO, M., 1993. New Zealand's Poisoned Paradise, *New Scientist*, 31 July, 29-33.
- URANO, K. *et al*, 1991. Adsorption of Chlorinated Organic Compounds on Activated Carbon from Water, *Wat. Res.*, 25, 1459-1464.
- VAN VLIET, B.M. and WEBER, W.J., 1981. Comparative Performance of Synthetic Adsorbents and Activated Carbon for Specific Compound Removal from Wastewaters, *J. Water Poll. Control. Fed.*, 53, 1585-1598.
- VAN VLIET, B.M. *et al*, 1980. Modelling and Prediction of Specific Compound Adsorption by Activated Carbon and Synthetic Adsorbents, *Wat. Res.*, 14, 1719-1728.
- WEBER, W.J. and LIU, K.T., 1980. Determination of Mass Transport Parameters for Fixed-Bed Adsorbers, *Chem. Eng. Commun.*, 6, 49-60.

- WEBER, W.J. and PIRBAZARI, M., 1982. Adsorption of Toxic and Carcinogenic Compounds from Water, *Jour. AWWA.*, April, 203-209.
- WEBER, T.W. and CHAKRAVORTI, R.K., 1974. Pore and Solid Diffusion Models for Fixed-Bed Adsorbers, *AIChE. J.*, 20, 228-237.
- WEBER, W.J. *et al*, 1991. Sorption Phenomena in Subsurface Systems: Concepts, Models and Effects on Contaminant Fate and Transport, *Wat. Res.*, 25, 499-528
- WEBER, W.J., 1984. Evolution of a Technology, *J. Env. Eng. Div.*, 110, 899-917.
- WEBER, W.J. and LIANG, S., 1983. A Dual Particle-Diffusion Model for Porous Adsorbents in Fixed Beds, *Environ. Prog.*, 2, 167-175.
- WEBER, W.J., 1972. *Physicochemical Processes for Water Quality Control*, Wiley Interscience, New York.
- WEBER, W.J. and WANG, C.K., 1987. A Microscale System for Estimation of Model Parameters for Fixed-Bed Adsorbers, *Environ. Sci. Technol.*, 21, 1096-1102.
- WEBER, W.J. and SMITH, E.H., 1987. Simulation and Design Models for Adsorption Processes, *Environ. Sci. Technol.*, 21, 1040-1050.
- WEBER, W.J. and SMITH, E.H., 1986. Removing Dissolved Organic Contaminants from Water, *Environ. Sci. Tech.*, 20, 970-979.

- WESTERMARK, M., 1975. Kinetics of Activated Carbon Adsorption, *J. Water Poll.Control Fed.*, 47, 704-719.
- WILKE, C.R. and CHANG, P., 1955. Correlation of Diffusion Coefficients in Dilute Solutions, *AIChE. J.*, 1, 264-270
- WONG, J. *et al*, 1992. Petroleum Effluent Toxicity Reduction - From Pilot to Full-Scale Plant, *Wat. Sci. Tech.*, 25, 221-228.
- WORLEY, 1992. *Potentially Contaminate Sites in New Zealand: A Broad Scale Assessment*. Report for the Ministry for the Environment.
- YING, W. *et al*, 1990. Adsorptive Capacities of Activated Carbon for Organic Constituents of Wastewaters, *Environ. Prog.*, 9, 1-9.

PCP Spectrophotometer Calibration Curve (22/7/94)



$$y=0.0136x$$

Equilibrium Isotherm 14: 26/7/94

PCP conc:	255 ppm
PCP vol:	100 ml
Temp:	25 C
Mean pH:	8.94

PCP Abs: 0.863

0.867 0.859 0.861 0.867 0.862

Flask Number	Mass Act. Carbon(g)	Equilibrium UVS Abs.	Equilibrium Conc (ppm)	Adsorbed Conc(mg/g)
1	0.0473	0.889	131	261.2
2	0.0634	0.805	119	214.4
3	0.0738	0.671	99	210.9
4	0.0823	0.796	59	238.2
5	0.0905	0.930	69	205.7
6	0.1052	0.795	59	186.4
7	0.1145	0.630	47	181.8
8	0.1259	0.490	36	173.5
9	0.1412	0.349	26	162.0
10	0.1489	0.263	20	157.9
11	0.1604	0.221	17	148.5
12	0.1709	0.168	13	141.7

pH	Spectrophotometer Readings			Mean Reading
8.29	0.887	0.89	0.891	0.889333
	0.692	0.692	0.693	0.804905
8.57	0.6	0.607	0.607	0.670844
8.94	1.03	1.027	1.027	0.795549
8.65	0.876	0.879	0.878	0.930364
9.03	0.663	0.667	0.669	0.794623
9.22	0.536	0.539	0.539	0.62966
9.09	0.401	0.394	0.392	0.490094
8.82	0.256	0.256	0.255	0.349156
9.29	0.241	0.242	0.244	0.263308
9.19	0.185	0.186	0.187	0.221187
9.26	0.134	0.131	0.134	0.168312

Equilibrium Isotherm 15: 27/7/94

PCP conc:	250 ppm
PCP vol:	100 ml
Temp:	25 C
Mean pH:	8.88

PCP Abs: 0.846

(25% dil) 0.845 0.846 0.848 0.846

Flask Number	Mass Act. Carbon(g)	Equilibrium UVS Abs.	Equilibrium Conc (ppm)	Adsorbed Conc(mg/g)
1	0.0472	0.759	112	291.8
2	0.0614	0.715	106	234.9
3	0.0712	0.645	95	216.9
4	0.0808	0.986	73	219.1
5	0.0918	0.927	68	197.6
6	0.1024	0.307	23	221.6
7	0.1107	0.570	42	187.5
8	0.1298	0.312	23	174.5
9	0.1424	0.241	18	162.8
10	0.1615	0.101	8	149.9
11	0.1733	0.117	9	139.0
12	0.1806	0.101	8	134.0

pH	Spectrophotometer Readings			Mean Reading
8.01	0.757	0.759	0.76	0.759
8.58	0.713	0.714	0.717	0.715
9.01	0.644	0.645	0.646	0.645
8.70	0.981	0.988	0.989	0.986
9.32	0.923	0.93	0.929	0.927
7.89	0.305	0.308	0.308	0.307
9.25	0.57	0.571	0.569	0.570
9.51	0.31	0.313	0.313	0.312
9.36	0.239	0.243	0.241	0.241
8.13	0.099	0.102	0.102	0.101
9.38	0.116	0.118	0.118	0.117
9.45	0.102	0.1	0.102	0.101

Equilibrium Isotherm 16: 28/7/94

PCP conc:	248 ppm
PCP vol:	100 ml
Temp:	25 C
Mean pH:	9.40

PCP Abs: 0.839

(25% dil) 0.838 0.84 0.84 0.839

Flask Number	Mass Act. Carbon(g)	Equilibrium UVS Abs.	Equilibrium Conc (ppm)	Adsorbed Conc(mg/g)
1	0.0528	0.772	114	253.2
2	0.0622	0.726	107	225.9
3	0.0758	0.613	91	207.3
4	0.0918	0.723	53	211.7
5	0.1027	0.673	50	192.8
6	0.1121	0.678	50	176.3
7	0.1313	0.380	28	167.2
8	0.1429	0.242	18	160.7
9	0.1556	0.151	11	151.9
10	0.1640	0.139	10	144.6
11	0.1746	0.114	9	136.9

pH	Spectrophotometer Readings			Mean Reading
9.23	0.773	0.772	0.772	0.772
8.93	0.724	0.726	0.728	0.726
9.05	0.613	0.613	0.612	0.613
8.68	0.722	0.724	0.722	0.723
9.26	0.671	0.675	0.674	0.673
9.75	0.677	0.679	0.678	0.678
9.85	0.378	0.38	0.381	0.380
9.57	0.241	0.242	0.243	0.242
9.77	0.15	0.151	0.151	0.151
9.71	0.137	0.14	0.14	0.139
9.60	0.113	0.114	0.114	0.114

Equilibrium Isotherm 17: 29/7/94

PCP conc:	499 ppm
PCP vol:	100 ml
Temp:	25 C
Mean pH:	

PCP Abs: 0.845 (12.5%) 0.846 0.845 0.844 0.844

Flask Number	Mass Act Carbon(g)	Equilibrium UVS Abs.	Equilibrium Conc (ppm)	Adsorbed Conc(mg/g)
1	0.1836	0.104	16	263.0
2	0.1912	0.381	57	231.2
3	0.2010	0.068	10	243.0
4	0.2111	0.174	26	223.8
5	0.2219	0.180	27	212.5
6	0.2352	0.098	15	205.6
7	0.2491	0.088	13	194.8
8	0.2889	0.036	6	183.3
9	0.3004	0.017	3	165.0
10	0.3252	0.039	6	151.4
11	0.3469	0.034	6	142.1
12	0.4034	0.018	3	122.8

pH	Spectrophotometer Readings			Mean Reading
	0.102	0.105	0.104	0.104
	0.378	0.382	0.385	0.381
	0.065	0.066	0.066	0.066
	0.177	0.174	0.172	0.174
	0.171	0.185	0.184	0.180
	0.098	0.099	0.098	0.098
	0.064	0.09	0.089	0.068
	0.037	0.039	0.031	0.036
	0.017	0.017	0.017	0.017
	0.038	0.039	0.04	0.039
	0.032	0.037	0.034	0.034
	0.014	0.02	0.021	0.018

Equilibrium Isotherm 18: 3/8/94

PCP conc:	499 ppm
PCP vol:	100 ml
Temp:	25 C
Mean pH:	9.84

PCP Abs: 0.845 (12.5%) 0.844 0.846 0.846 0.844

Flask Number	Mass Act Carbon(g)	Equilibrium UVS Abs.	Equilibrium Conc (ppm)	Adsorbed Conc(mg/g)
1	0.1014	1.618	238	256.9
2	0.1209	1.409	208	240.9
3	0.1313	1.251	184	239.5
4	0.1405	1.188	172	232.5
5	0.1504	1.702	125	248.3
6	0.1602	1.693	125	233.5
7	0.1706	1.599	118	223.4
8	0.1805	1.395	103	219.4
9	0.1882	1.396	103	210.4
10	0.1906	1.135	84	217.8
11	0.2004	0.974	72	213.0

pH	Spectrophotometer Readings			Mean Reading	
9.61	(50% dil)	1.616	1.619	1.619	1.618
9.92	(50% dil)	1.41	1.41	1.407	1.409
9.89	(50% dil)	1.25	1.252	1.25	1.251
10.08	(50% dil)	1.187	1.189	1.188	1.188
9.24		1.702	1.702		1.702
9.78		1.691	1.694	1.694	1.693
10.12		1.599	1.599		1.599
10.14		1.394	1.395		1.395
9.65		1.398	1.398	1.391	1.396
9.48		1.134	1.135		1.135
10.30		0.974	0.974		0.974

Equilibrium Isotherm 19: 4/8/94

PCP conc:	506 ppm
PCP vol:	100 ml
Temp:	25 C
Mean pH:	10.29

PCP Abs: 0.858 (12.5%) 0.854 0.861 0.857 0.859

Flask Number	Mass Act Carbon(g)	Equilibrium UVS Abs.	Equilibrium Conc (ppm)	Adsorbed Conc(mg/g)
1	0.4022	0.068	5	124.8
2	0.3413	0.123	9	145.6
3	0.2948	0.218	16	186.2
4	0.2777	0.252	19	175.5
5	0.2428	0.569	42	191.2
6	0.2255	0.773	57	199.2
7	0.2171	0.827	61	205.1
8	0.2071	0.985	73	209.4
9	0.1911	0.634	84	215.9
10	0.1843	0.615	91	225.4
11	0.1763	0.713	105	227.5

pH	Spectrophotometer Readings			Mean Reading	
10.40		0.067	0.068	0.068	0.068
10.34		0.123	0.122		0.123
10.57		0.218	0.218		0.218
10.02		0.252	0.251	0.252	0.252
10.45		0.568	0.569		0.569
10.40		0.773	0.773		0.773
10.38		0.826	0.827		0.827
10.37		0.985	0.985		0.985
10.24	(50% dil)	0.634	0.635	0.633	0.634
9.71	(50% dil)	0.615	0.615	0.615	0.615
10.26	(50% dil)	0.713	0.712	0.713	0.713

Equilibrium Isotherm 20: 8/8/94

PCP conc:	497 ppm
PCP vol:	100 ml
Temp:	25 C
Mean pH:	119.01

PCP Abs: 0.842 (12.5%) 0.842 0.84 0.842 0.844 0.842

UVS Results

HPLC Results

Flask Number	Mass Act. Carbon(g)	Equilibrium UVS Abs.	Equilibrium Conc (ppm)	Adsorbed Conc(mg/g)	Equil. Conc(ppm)	Adsorbed Conc(mg/g)
1	0.3689	0.070	5	123.2	3.2	123.8
2	0.3480	0.085	7	140.9	4.2	141.8
3	0.2994	0.218	18	160.8	14.9	161.0
4	0.2654	0.324	24	178.2	23.8	178.4
5	0.2477	0.530	39	184.8	38.5	185.1
6	0.2292	0.595	44	197.7	43.4	197.9
7	0.2126	0.941	69	201.1	70.8	200.5
8	0.2031	0.951	70	210.2	72	209.3
9	0.1919	0.663	98	208.0	95.1	208.4
10	0.1836	0.692	102	215.1	101.9	215.2
11	0.1755	0.710	105	223.4	105.3	223.2

Spectrophotometer Readings			Mean Reading
0.068	0.069	0.072	0.070
0.083	0.086	0.086	0.085
0.216	0.218	0.219	0.218
0.323	0.325	0.325	0.324
0.527	0.53	0.532	0.530
0.591	0.597	0.597	0.595
0.936	0.942	0.945	0.941
0.952	0.951	0.951	0.951
0.662	0.664	0.662	0.663
0.69	0.693	0.692	0.692
0.708	0.712	0.71	0.710

Exp 3: 23 Sept 1994		
Volume:	3000 ml	
Carbon:	3.999 g	
Stirrer:	180 rpm	
Samples:	0.6 ml	
Time (s)	Time (min)	Conc (mg/l)
0	0	240.6
10	0.1666667	235.8
20	0.3333333	234.9
30	0.5	233.4
40	0.6666667	232.3
50	0.8333333	231
60	1	
70	1.1666667	
80	1.3333333	229.4
90	1.5	
100	1.6666667	225
110	1.8333333	
120	2	225.7
	3	221.4
	4	221.8
	5	216.6
	10	204.7
	20	195
	30	182.8
	40	176.2
	50	171.2
	60	161
	90	149.8
	120	141.5
	180	125.5
	240	
	302	104.6
	360	97.38
	430	89.66
sep. fact:	0.7081229	
kl A/V:	0.0005226	
kl:	0.0038421 cm/s	
BF/3:	75	
Bi:	317.74144	
R2/Ds:	611147.33 s	
Ds:	2.150E-09 cm ² /s	

Exp 4: 27 Sept 1994		
Volume:	3000 ml	
Carbon:	4 g	
Stirrer:	390 rpm	
Samples:	0.6 ml	
Time (s)	Time (min)	Conc (mg/l)
0	0	232.7
10	0.1666667	229.3
20	0.3333333	228.1
30	0.5	225.2
40	0.6666667	224
50	0.8333333	222.7
60	1	
70	1.1666667	
80	1.3333333	219.5
90	1.5	
100	1.6666667	218.5
110	1.8333333	
120	2	217
	3	212.4
	4	209.2
	5	206.1
	10	194.4
	20	181.2
	30	163
	40	159.4
	50	152.1
	60	145.5
	90	134.7
	120	125
	171	109.8
	236	95.25
	300	84.15
	360	72.74
	420	63.68
sep. fact:	0.6888278	
kl A/V:	0.000674	
kl:	0.00495 cm/s	
BF/3:	90	
Bi:	391.97022	
R2/Ds:	581443.6 s	
Ds:	2.26E-09 cm ² /s	

Exp 5: 29 Sept 1994		
Volume:	3000 ml	
Carbon:	4 g	
Stirrer:	560 rpm	
Samples:	0.6 ml	
Time (s)	Time (min)	Conc (mg/l)
0	0	243.8
10	0.1666667	234.7
20	0.3333333	233.6
30	0.5	231.5
40	0.6666667	227.7
50	0.8333333	227.3
60	1	225.3
70	1.1666667	224.1
80	1.3333333	218.9
90	1.5	
100	1.6666667	223
110	1.8333333	
120	2	220.1
	3	220.3
	4	211.8
	5	
	10	178
	20	164.7
	30	159
	40	147
	50	139.3
	60	
	90	117
	121	108.6
	185	96.37
	245	79.72
	301	61.82
	363	53.72
	420	39.53
sep. fact:	0.7156576	
kl A/V:	0.000819	
kl:	0.0060192	cm/s
BF/3:	100	
Bi:	419.19487	
R2/Ds:	281032.84	s
Ds:	4.676E-09	cm ² /s

Exp 6: 30 Sept 1994		
Volume:	3000 ml	
Carbon:	4 g	
Stirrer:	760 rpm	
Samples:	0.6 ml	
Time (s)	Time (min)	Conc (mg/l)
0	0	244.1
10	0.1666667	241.3
20	0.3333333	235.1
30	0.5	233
40	0.6666667	227.75
50	0.8333333	232.1
60	1	230.6
70	1.1666667	222.4
80	1.3333333	
90	1.5	224
100	1.6666667	
110	1.8333333	222.6
120	2	221.7
	3	223.7
	4	222.5
	5	213.9
	10	203.2
	20	188.8
	30	175.4
	40	
	50	157.4
	60	149.9
	90	124.5
	120	
	180	82.89
	253	66.81
	300	57.75
	360	44.86
	420	37.21
sep. fact:	0.71638	
kl A/V:	0.001737	
kl:	0.012764	cm/s
BF/3:	65	
Bi:	272.202	
R2/Ds:	272346.4	s
Ds:	4.83E-09	cm ² /s

Adsorption Column Run 3Fluid Properties:

Density:	1000	kg/m ³
Viscosity:	0.001	kg/ms
Critical vol:	484.8	cm ³ /gmol

Adsorbent Properties:

Particle Dia:	0.0725	cm
Particle Den:	0.811	g/cm ³

Experimental Parameters:

Feed Conc:	200	mg/L
Temperature:	298	K
Flow Rate:	6.15	ml/min
Col Diameter:	1	cm
Col Length:	6.3	cm
Mass Carbon:	2.44	g
Loading Rate:	30.22	mg/g/hr
Bed Porosity:	0.39	
Inters. vel:	0.33	cm/s
Residence Time:	18.91	s

Model Parameters:

K:	95	
1/n:	0.18	
Surface Dif Cof:	2.26E-09	cm ² /s
Diffusivity:	3.69E-06	cm ² /s
Reynolds No:	2.416	
Schmidt No:	2709	
Disp. Coeff:	0.070026	cm ² /s (Fried)
	0.04832	cm ² /s (Levenspiel)
Film Coeff:	0.001554	cm/s (Gnielinski)
	0.001940	cm/s (Wilson & Geankoplis)
	0.001786	cm/s (Williamson et al)
Peclet No:	43	
Ps	24921	
Bet	30756	
Sigma:	1000	
Rf:	1554	
Bi:	24.9	

Adsorption Column Run 4Fluid Properties:

Density:	1000	kg/m ³
Viscosity:	0.001	kg/ms
Critical vol:	484.8	cm ³ /gmol

Adsorbent Properties:

Particle Dia:	0.0725	cm
Particle Den:	0.811	g/cm ³

Experimental Parameters:

Feed Conc:	199	mg/L
Temperature:	298	K
Flow Rate:	2.80	ml/min
Col Diameter:	1	cm
Col Length:	6.3	cm
Mass Carbon:	2.47	g
Loading Rate:	13.53	mg/g/hr
Bed Porosity:	0.38	
Inters. vel:	0.15	cm/s
Residence Time:	40.71	s

Model Parameters:

K:	95	
1/n:	0.18	
Surface Dif Cof:	2.26E-09	cm ² /s
Diffusivity:	3.69E-06	cm ² /s
Reynolds No:	1.12	
Schmidt No:	2709	
Disp. Coeff:	0.027896	cm ² /s (Fried)
	0.022439	cm ² /s (Levenspiel)
Film Coeff:	0.001128	cm/s (Gnielinski)
	0.001522	cm/s (Wilson & Geankoplis)
	0.001349	cm/s (Williamson et al)
Peclet No:	43	
Ps	18086	
Bet	14283	
Sigma:	1004	
Rf:	1610	
Bi:	18.0	

Adsorption Column Run 5Fluid Properties:

Density:	1000 kg/m ³
Viscosity:	0.001 kg/ms
Critical vol:	484.8 cm ³ /gmol

Adsorbent Properties:

Particle Dia:	0.0725 cm
Particle Den:	0.811 g/cm ³

Experimental Parameters:

Feed Conc:	200 mg/L
Temperature:	298 K
Flow Rate:	5.07 ml/min
Col Diameter:	1 cm
Col Length:	6.3 cm
Mass Carbon:	2.31 g
Loading Rate:	26.24 mg/g/hr
Bed Porosity:	0.42
Inters. vel:	0.25 cm/s
Residence Time:	24.78 s

Model Parameters:

K:	95	
1/n:	0.18	
Surface Dif Cof:	2.26E-09 cm ² /s	
Diffusivity:	3.692E-06 cm ² /s	
Reynolds No:	1.84	
Schmidt No:	2709	
Disp. Coeff:	0.0506075 cm ² /s	(Fried)
	0.0368628 cm ² /s	(Levenspiel)
Film Coeff:	0.0016993 cm/s	(Gnielinski)
	0.0016829 cm/s	(Wilson & Geankoplis)
	0.0017608 cm/s	(Williamson et al)
Peclet No:	43	
Ps	27257	
Bet	23463	
Sigma:	1001	
Rf:	1365	
Bi:	27.2	